NASA/TM–2009-215942

Shuttle Gaseous Hydrogen Venting Risk from Flow Control Valve Failure

J. Philip Drummond, Robert A. Baurle, Richard L. Gafney, Andrew T. Norris,
Gerald L. Pellett, and Kenneth E. Rock
NASA Langley Research Center, Hampton, Virginia

October 2009

NASA STI Program . . . in Profile

Since its founding, NASA has been dedicated to the advancement of aeronautics and space science. The NASA scientific and technical information (STI) program plays a key part in helping NASA maintain this important role.

The NASA STI program operates under the auspices of the Agency Chief Information Officer. It collects, organizes, provides for archiving, and disseminates NASA's STI. The NASA STI program provides access to the NASA Aeronautics and Space Database and its public interface, the NASA Technical Report Server, thus providing one of the largest collections of aeronautical and space science STI in the world. Results are published in both non-NASA channels and by NASA in the NASA STI Report Series, which includes the following report types:

- TECHNICAL PUBLICATION. Reports of completed research or a major significant phase of research that present the results of NASA programs and include extensive data or theoretical analysis. Includes compilations of significant scientific and technical data and information deemed to be of continuing reference value. NASA counterpart of peer-reviewed formal professional papers, but having less stringent limitations on manuscript length and extent of graphic presentations.

- TECHNICAL MEMORANDUM. Scientific and technical findings that are preliminary or of specialized interest, e.g., quick release reports, working papers, and bibliographies that contain minimal annotation. Does not contain extensive analysis.

- CONTRACTOR REPORT. Scientific and technical findings by NASA-sponsored contractors and grantees.

- CONFERENCE PUBLICATION. Collected papers from scientific and technical conferences, symposia, seminars, or other meetings sponsored or co-sponsored by NASA.

- SPECIAL PUBLICATION. Scientific, technical, or historical information from NASA programs, projects, and missions, often concerned with subjects having substantial public interest.

- TECHNICAL TRANSLATION. English-language translations of foreign scientific and technical material pertinent to NASA's mission.

Specialized services also include creating custom thesauri, building customized databases, and organizing and publishing research results.

For more information about the NASA STI program, see the following:

- Access the NASA STI program home page at *http://www.sti.nasa.gov*

- E-mail your question via the Internet to help@sti.nasa.gov

- Fax your question to the NASA STI Help Desk at 443-757-5803

- Phone the NASA STI Help Desk at 443-757-5802

- Write to:
  NASA STI Help Desk
  NASA Center for AeroSpace Information
  7115 Standard Drive
  Hanover, MD 21076-1320

NASA/TM–2009-215942

Shuttle Gaseous Hydrogen Venting Risk from Flow Control Valve Failure

J. Philip Drummond, Robert A. Baurle, Richard L. Gafney, Andrew T. Norris,
Gerald L. Pellett, and Kenneth E. Rock
NASA Langley Research Center, Hampton, Virginia

National Aeronautics and
Space Administration

Langley Research Center
Hampton, Virginia 23681-2199

October 2009

Available from:

NASA Center for AeroSpace Information
7115 Standard Drive
Hanover, MD 21076-1320
443-757-5802

Abstract

This paper describes a series of studies to assess the potential risk associated with the failure of one of three gaseous hydrogen flow control valves in the orbiter's main propulsion system during the launch of Shuttle Endeavour (STS-126) in November 2008. The studies focused on critical issues associated with the possibility of combustion resulting from release of gaseous hydrogen from the external tank into the atmosphere during assent. The Shuttle Program currently assumes hydrogen venting from the external tank will result in a critical failure. The current effort was conducted to increase understanding of the risk associated with venting hydrogen given the flow control valve failure scenarios being considered in the Integrated In-Flight Anomaly Investigation being conducted by NASA.

1 Introduction

During the launch of Shuttle Endeavour (STS-126) in November 2008, one of three gaseous hydrogen flow control valves in the orbiter's main propulsion system failed to perform as designed. These valves function to maintain appropriate pressure levels within the external tank and to assure a steady flow of fuel to the main engines during assent. A drawing of the valve is shown in Figure 1. Inspections following return of the Shuttle showed that the valve poppet in one valve had failed as shown in Figure 2, possibly allowing debris from the poppet to travel down tubing that carries gaseous hydrogen from the Shuttle's main engines to the external tank. Had the poppet failure been larger, or had two valves simultaneously failed, gaseous hydrogen may have been released from a vent located on the surface of the external tank, subsequently mixing with atmospheric air and posing a possible risk of combustion on the surface of the external tank. The other two flow control valves did maintain the external tank ullage pressure within the nominal pressure control band during launch, preventing the release of hydrogen.

This paper considers critical issues associated with the possibility of combustion resulting from release of gaseous hydrogen from the external tank into the atmosphere during assent. As part of the NASA Integrated In-Flight Anomaly (IIFA) Investigation considerations, one of the integrated system effects that could result from future flow control valve failures, as noted above for the flight of STS-126, is hydrogen venting from the external tank intertank relief valve. The Shuttle Program currently assumes hydrogen venting from the external tank prior to 120 seconds after launch will result in a critical failure. The goal of the present effort is to increase understanding of the risk associated with venting hydrogen given the flow control valve failure scenarios being considered in the IIFA investigation.

2 Background

Failure of two gaseous hydrogen flow control valves or a larger poppet failure of a single valve could result in the release of hydrogen into the flow field around the external tank as shown in Figure 3. For comparison, streamlines tracing a typical path of hydrogen at two flight Mach numbers ($M = 0.3$, red and $M = 0.6$, blue) are shown in the figure. The hydrogen would be released from a 7 inch diameter vent pipe embedded in a shallow cavity as shown in Figure 4. The fuel would penetrate transversely into the air flowing about the external tank and then undergo turbulent mixing as the flow progresses downstream. Fuel-air mixing could also occur in the vent pipe cavity, and if proper conditions exist, the cavity could serve as an initial location for ignition and flame-holding on the surface of the external tank. The mixing process would continue with the remaining hydrogen, again providing a potential for ignition and combustion downstream under appropriate conditions. Critical conditions for ignition must therefore be determined.

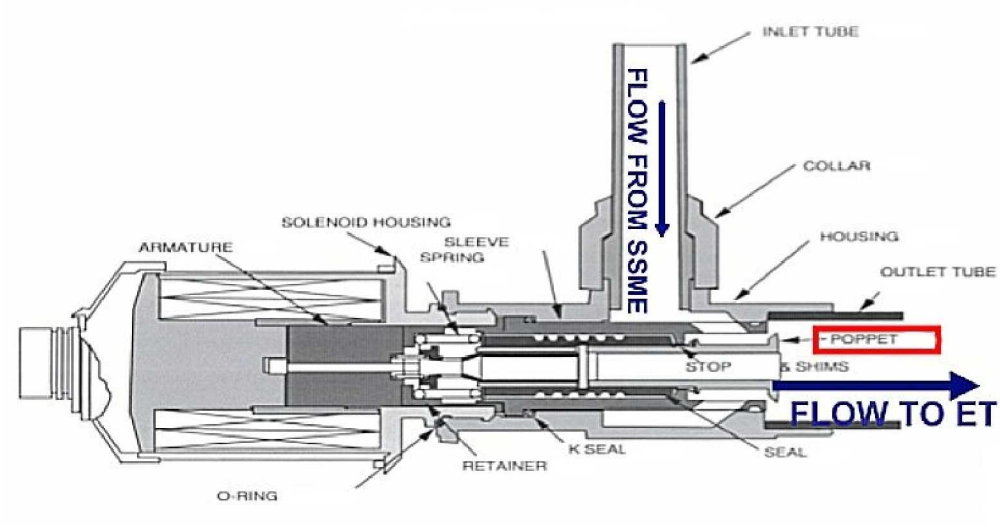

Figure 1. Orbitor main propulsion system gaseous hydrogen flow control valve.

Figure 2. Poppet head breakage of gaseous H_2 flow control valve on STS-126.

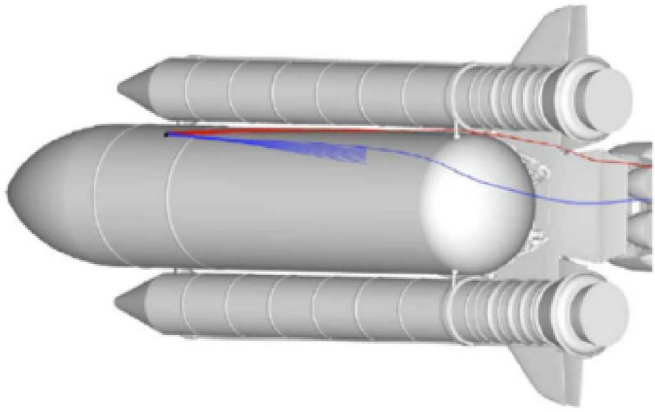

Figure 3. Vent location and hydrogen release streamlines.

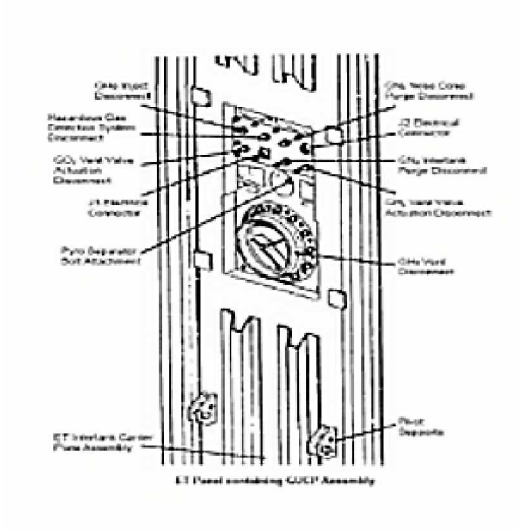

Figure 4. Detailed view of hydrogen vent on the surface of the external tank.

Ignition and reaction are a function of pressure, temperature and species concentrations. For combustion to take place, the proper combination of these variables must exist for a sufficient time to allow ignition to occur. Initially, hydrogen fuel and the external air must mix within a range of combustible proportions. If the mixture is too rich or lean, it will not ignite and burn. Second, there must be an ignition mechanism. If the temperature is high enough, the mixture will auto-ignite. If it is not sufficiently high, an ignition source is required. This source could be a hot spot created by a shock reflection, the exhaust plume of the solid rocket booster (SRB) or main engines, the firing of explosive bolts at SRB separation, lightning strikes, or possibly static discharge if such a discharge would provide sufficient energy over the necessary period of time. If the mixture does ignite, it must be determined whether the resulting flame propagates through the mixture or anchors itself at some location in the flow structure. If it propagates, the flame will move either as a detonation (supersonic flame propagation) or a deflagration (subsonic flame propagation).

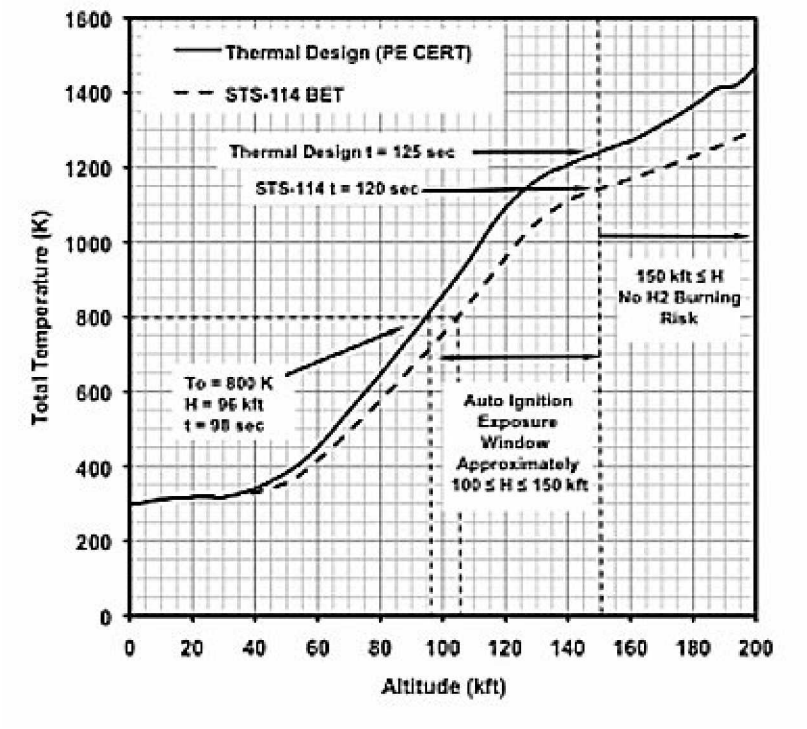

Figure 5. Approximate times for potential auto ignition based on Shuttle ascent thermal design trajectory.

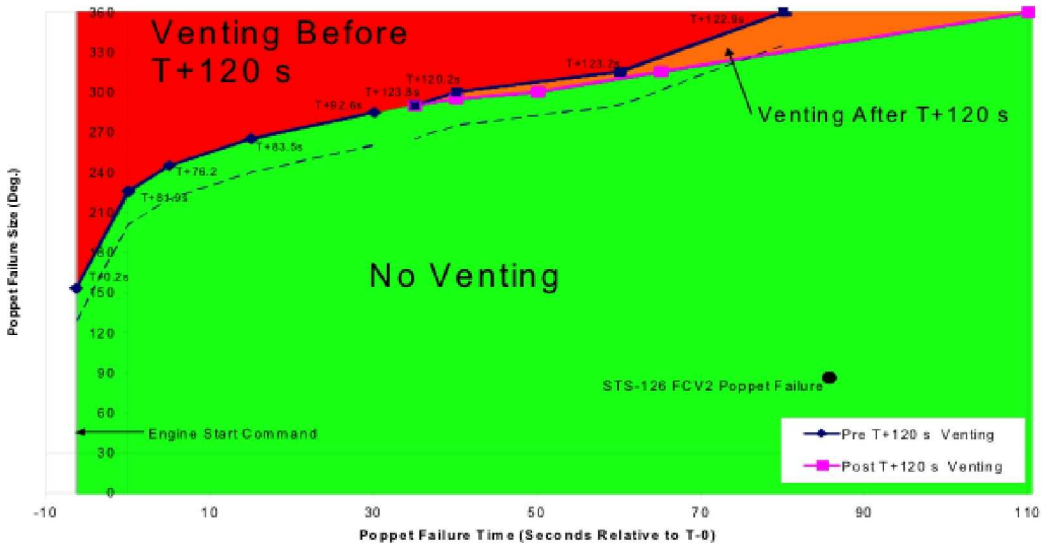

Figure 6. Exposure windows for a single poppet failure causing H_2 venting.

A detonation is a very strong combustion wave which travels at supersonic speeds with respect to the mixture through which it is propagating. The direct initiation of a detonation

wave requires a large amount of energy. In the case of the shuttle, the required energy levels are generally not available other than possibly the firing of an explosive bolt or a lightning strike. Detonations can be established with lower energy levels in confined spaces or if a deflagration wave accelerates to a detonation wave. In the case of the shuttle, a stream of hydrogen flowing over the external tank is only confined on one side by the tank itself. However, the presence of a solid surface can aid in the transition of a deflagration to a detonation through the production of turbulence and the reflection of pressure waves. Unfortunately, the process of deflagration to detonation transition is complex and depends heavily on the geometry and flow conditions. In the case of the shuttle, a further study with the specific geometry and flow conditions is required to better determine if a deflagration could transition to a detonation. Without detonation, once the Shuttle reaches supersonic speeds, the only mechanism for upstream flame propagation is through the subsonic portion of the boundary layer, very near the surface of the external tank. Furthermore, velocity gradients in the flowfield affect flame propagation. High cross-flow gradients stretch the flame front causing extinction of combustion. For steady localized burning on the surface of the external tank, the flame must be anchored by a favorable flow structure such as recirculation near the jet exit, a reflected shockwave or an irregularity (e.g. a bump, raised structure or cavity) in the surface of the external tank. The location of the flameholding is also likely to be the region of highest temperature due to external burning.

As indicated previously, external release of hydrogen gas during launch has been considered a mechanism for catastrophic failure during launch throughout the life of the Shuttle. The problem was first discussed in an April 6, 1967 memo from Werner Dahm [1], indicating that *"hydrogen venting below 10 kft be avoided; venting between 10 and 90 kft not be condoned as routine practice; between 90 and 160 kft be allowed; and above 160 kft no restrictions be imposed."* Prior studies had established a time line for potential auto ignition of released hydrogen based on Shuttle ascent thermal design trajectory [2] as shown in Figure 5. Based on later analyses, an exposure window for a single poppet failure was established. This window, giving venting limitations, is diagrammed in Figure 6 showing poppet failure time relative to launch as a function of poppet failure size. Pre- and post venting relative to a time of T + 120 s (with T being launch time) are given on the plot along with the time and size of the STS-126 poppet failure.

The intent of the analyses described in this paper is to determine the potential for combustion resulting from ignition of a gaseous hydrogen release due to a flow control valve failure. These analyses will then allow confirmation of the venting risk time displayed in Figure 6, or possibly move the T + 120 seconds time of concern to earlier in the flight. The remainder of this paper will describe the analyses used to make this determination.

3 Shuttle Hydrogen Vent Analyses

To analyze the Shuttle hydrogen vent problem, several approaches ranging from the use of empirical correlations to state-of-the-art numerical simulations were deemed appropriate. This approach allows some analyses to be completed in timely fashion while the more sophisticated analyses were conducted over a longer period of time. Additionally, each approach is used as a "sanity check" on the analyses to follow. To choose the methods of approach, the issues to be addressed in the analyses were first defined. The questions to be answered included:

1. Will vented gaseous H_2 auto-ignite?

2. Will vented gaseous H_2 be ignited by the solid rocket booster and/or the space Shuttle main engine plumes based on gaseous H_2 - air mixture concentrations?

3. Will vented gaseous H_2 be ignited from other sources (lightning, static discharge, etc.)?

4. Will burning gaseous H_2 propagate forward from base of external tank, assuming the solid rocket booster and/or the space Shuttle main engine plumes ignite the gaseous H_2?

5. If the mixture does ignite, will the flame propagate through the mixture or anchor itself at some flow structure (i.e. hot spot)?

6. If combustion occurs and is sustained, what are the heating rates from burning gaseous H_2 on the thermal protection system using CFD?

To determine if these events occur, four approaches were chosen to analyze the gaseous hydrogen release and its mixing with the external air flow. These approaches included:

1. A well stirred reactor analysis to determine the H_2 - air ignition time as a function of temperature, pressure, and species concentration

2. A jet mixing analysis to estimate gaseous H_2 - air concentrations and plume size downstream of the hydrogen vent

3. A flashback analysis to address the potential for flame propagation from a point of ignition, i.e. the solid rocket booster and/or the space Shuttle main engine plumes, forward in the boundary layer of the external tank

4. A three-dimensional analysis of the flow field using the VULCAN Navier-Stokes code with detailed finite rate chemistry. Later analyses may also include the coupled effect of turbulence and chemistry on the flow field.

Each of these approaches will now be described in more detail and preliminary results will be given where possible to provide initial answers to the questions posed in this discussion.

3.1 Well Stirred Reactor Analysis

An analysis to determine the potential for auto-ignition during any point of the ascent trajectory was conducted using well stirred reactor theory [3]. This analysis does not consider the velocity field of the flow convecting the hydrogen and air mixture, but it does allow for the use of full complex kinetic mechanisms. Hence, the methodology is ideal for performing a quick and conservative (provided that conditions are chosen appropriately) assessment of the potential for auto-ignition. The SENKIN module of the CHEMKIN software package was used to predict the auto-ignition time for a hydrogen-air mixture given initial conditions for the temperature, pressure, and stoichiometry of the mixture. The SENKIN program integrates the ordinary differential equations that describe the conservation of species mass and energy as a function of time. Details describing the code are given in Reference 4.

The potential for auto-ignition at any point along the ascent trajectory was determined by first defining bounding limits for the initial conditions required to perform the point kinetics analyses. The bounding limits that were chosen were based on the following observations:

1. The potential for auto-ignition is maximized when the chemical constituents are near stoichiometric proportions

2. In the absence of an ignition source, the highest local temperature that can be present is the freestream total temperature

3. The pressure was assumed to be the freestream pressure. (Peak local pressure conditions could be employed as a less-conservative assumption, but as the analysis will show, the auto-ignition behavior is not sensitive to pressure over a large fraction of the trajectory.)

4. In the absence of any "large" recirculation zones, auto-ignition must occur at a time scale that is smaller than the flow residence time (proportional to L/U). A constant scaling factor (> 1) can be used to account for separated zones.

The procedure to obtain the auto-ignition limits involved the following iterative analysis to be performed at each trajectory point. Given a stoichiometric mixture, freestream pressure, and the bounding residence time, a guess is made for the temperature that will result in an ignition delay that matches the supplied residence time. The SENKIN module is executed to extract the ignition delay. The ignition delay is extracted from the time history of the temperature rise due to reaction. A sample output from SENKIN is given in Figure 7. There are a variety of different options for defining the ignition delay. Popular choices include the time required to achieve some percentage of the temperature rise due to combustion or the time where the temperature gradient is a maximum. The latter choice was used in this effort. The initial temperature is iterated upon until the ignition delay time that is extracted matches the bounding value given by the supplied residence time.The hydrogen air kinetic model used for this analysis was the model of Li et al. [5]

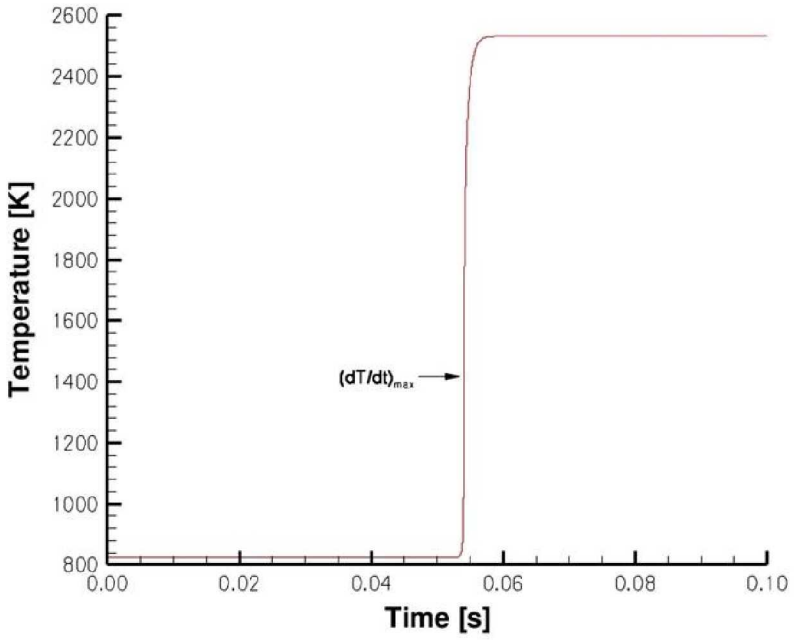

Figure 7. Typical temporal history of temperature output from SENKIN (used todefine the ignition delay time).

The above analysis was performed along the entire trajectory starting from MET = 10 seconds and ending at MET = 130 seconds in 10 second intervals. The results extracted from this analysis are displayed in Figure 8. In this figure, the Shuttle trajectory points (in terms of freestream total temperature as a function of freestream pressure) are plotted as the red curve. The auto-ignition bound at each trajectory point based on the analysis outlined above is plotted as the blue curve. These results indicate that auto-ignition is not likely

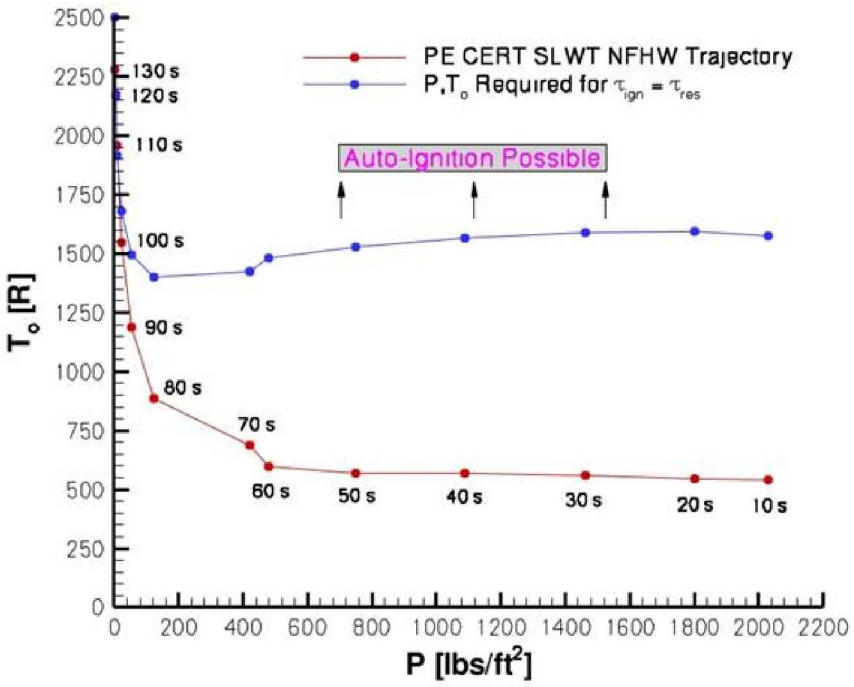

Figure 8. Auto-ignition bound estimate along the ascent trajectory.

to occur for MET $<$ 100 seconds or for MET $>$ 130 seconds. The use of an ignition delay definition based on the maximum temperature gradient turns out to be a conservative choice (conservative in the sense that the resulting ignition delay time is lower than that given by other choices that are based on a percentage of the temperature rise due to combustion) at the relatively low pressures that occur at MET $>$ 100. Hence, the convergence of the two curves between 100 and 130 seconds is to some extent a result of the choice used to define the ignition delay time. It is interesting to note that the auto-ignition bounds that resulted from this analysis are practically identical to the results from the less rigorous analysis used to generate Figure 5. Both analyses show that the window between roughly 100 and 130 seconds to be the most likely trajectory range that could support auto-ignition.

3.2 Jet Mixing Analysis

As a first order approach to analyze the direction and mixing of the hydrogen plume exiting the external tank following a hydrogen flow control valve failure, an empirical relationship was utilized to predict the spread of a transverse jet into a cross-flow. This approach provides an estimate of the hydrogen plume width and concentration as a function of downstream distance. From this information, regions where the hydrogen to air ratio is sufficient to support combustion can be predicted. This analysis can be performed quickly, and applied to a variety of flight conditions and hydrogen vent rates.

The JETPEN code [6] provides the required empirical model. The code is based on the similarity between a jet discharging into a quiescent medium and a jet discharging into a cross-flow. Correlations allow the calculation of the complete trajectory of the jet as well as the properties of the jet such as bulk H_2 mass concentration. Details of the modeling are

Time	vent	mass flow	Pt	Tt	M
MET = 55	5 inch	2.668	17.78	220.6	2.14
	choked	1.334	8.89	220.6	2.14
	7 inch	2.668	42.24	220.6	3.11
	isentropic	1.334	21.12	220.6	3.11
MET = 75	5 inch	2.272	15.73	223.2	2.14
	choked	1.136	7.87	223.2	2.14
	7 inch	2.272	37.37	223.2	3.11
	isentropic	1.136	18.69	223.2	3.11

Table 1. Calculated hydrogen jet exit conditions.

provided by Billig et al. [6]

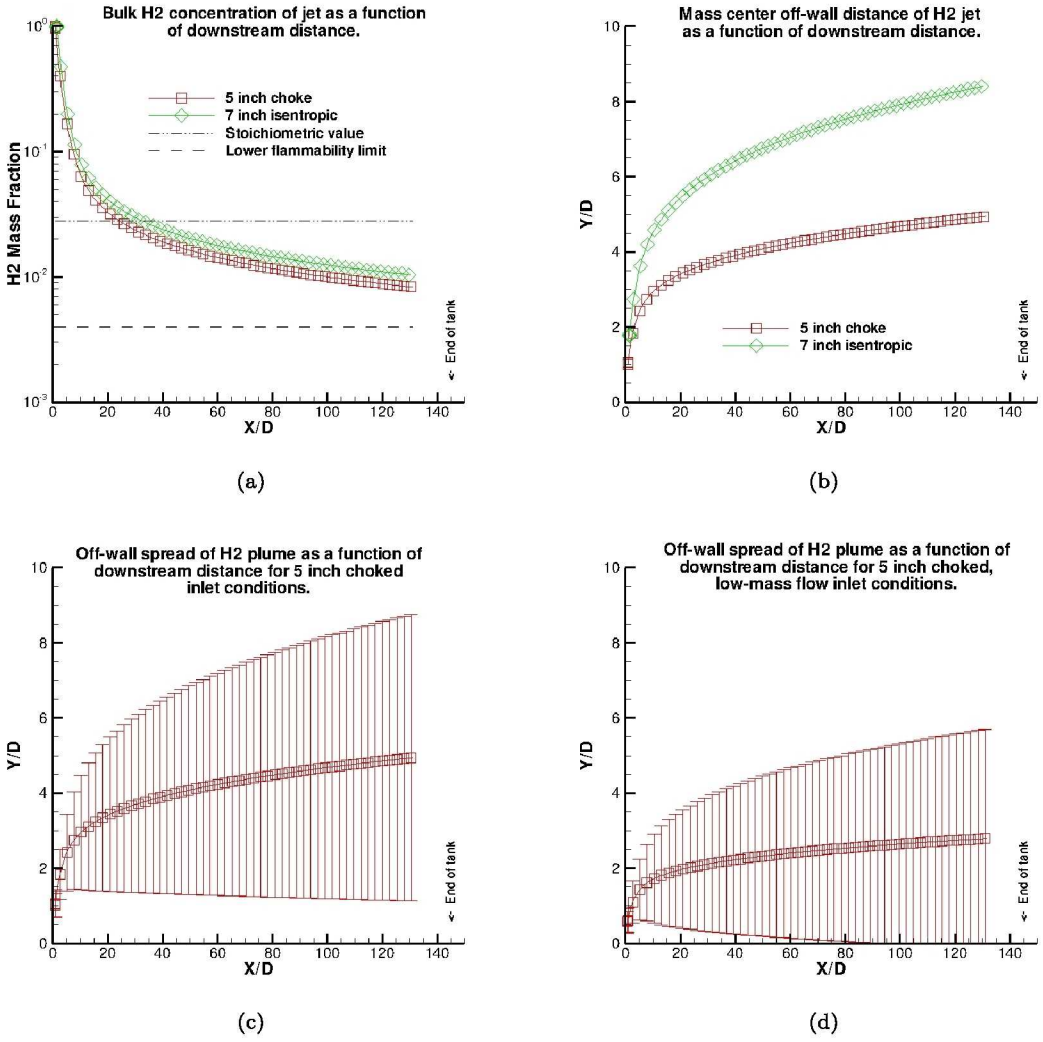

Figure 9. MET = 55 JetPen Results.

Two flight conditions were chosen for the analysis corresponding to a Mission Elapsed

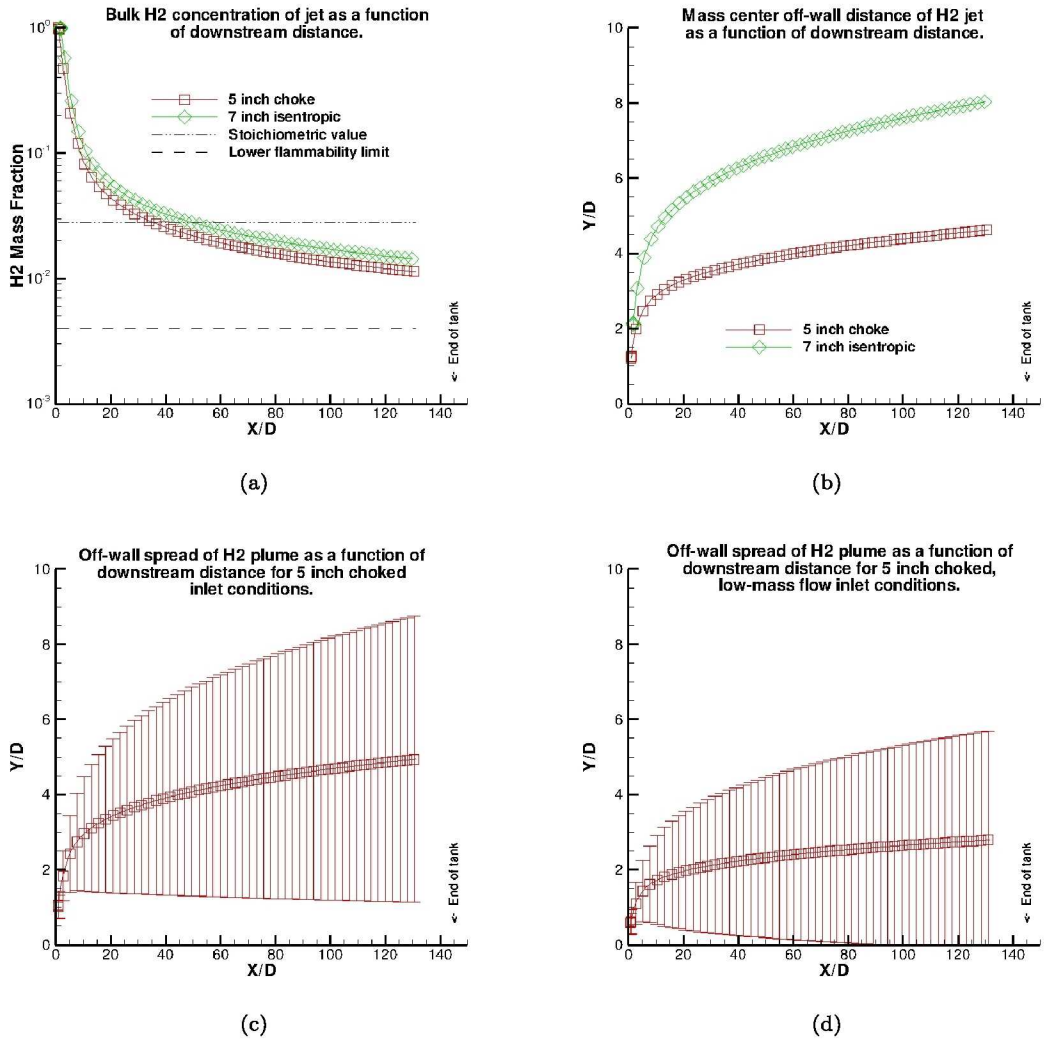

Figure 10. MET = 75 JetPen Results.

Time (MET) of 55 and 75 seconds [7]. At both of these times, several different assumptions about the venting process were considered. One assumption was that the vent pipe was choked at the pressure relief valve, and again where the vent suddenly expanded from 5 inches to 7 inches diameter. Then the hydrogen expands isentropically to the 7-inch diameter section at the exit. The other condition considered was that the hydrogen just expands isentropically from the pressure relief valve to the 7-inch diameter section. In addition to the specified mass flow which had been provided for all of these conditions, further simulations were performed with the mass flow of hydrogen halved. Physical properties of the jet at the exit, such as density and temperature were obtained using the STANJAN code [9]. Values obtained for the cases are shown in Table 1. The venting conditions and external flow conditions were then used as an input to JETPEN, and the resulting jet shapes and concentration profiles were obtained.

Shown in Figure 9 are the results for the MET = 55 conditions. The bulk concentrations of H2 for both the 5-inch choked and 7-inch expansion cases are shown to be pretty close in

the top left figure. Also it should be noted that both jet conditions result in a combustable mixture of hydrogen propagating all the way to the end of the tank. As expected, the jet penetration distance is shown to be significantly larger for the 7-inch isentropic expansion case in the top-right figure. The two lower figures show the plume width for the full and half mass flow cases for the 5-inch choked vent condition. As can be seen the lower mass flow gives less penetration, and also has the plume descending all the way to the tank surface, unlike the full mass flow which stays above the boundary layer.

In Figure 10 the results are shown for the MET = 75 seconds. Comparisons with the MET = 55 second results show very little change in the results, again with a combustable mixture of hydrogen propagating all the way down the tank, and the lower mass flow plume reaching the tank surface.

In conclusion, this analysis shows that for MET = 55 and 75 seconds, the vent plume has a sufficiently high concentration of hydrogen to support combustion from the vent location all the way to the end of the tank. For the flame to propagate upstream, however, even in a favorable fuel-air mixture, the flame speed (the rate at which a flame can propagate in a laminar or turbulent mixture) must exceed the downstream velocity of the flow. Due to the flow velocities just away from the surface of the external tank, the flame speed can only exceed the flow velocity in the boundary layer near the tank surface. In addition to the constraint on flame speed, for a flame propagating in the boundary layer to persist, it must also be in a favorable environment in which local velocity gradients are not too severe. Strong velocity gradients can cause radicals important to the combustion process to be stripped away resulting in flame extinction. The effects of flame speed and flame extinction are discussed in the next section.

3.3 Flashback Analysis

A relatively simple flashback analysis was employed to identify possible hydrogen-venting-with-combustion hazards during the Space Shuttle subsonic ascent [10]. The analysis identifies conditional potentials for stable combustion of vented-hydrogen with ambient air in the boundary layer of the Shuttle External Tank, presuming an ignition / flame-piloting source. The objective was to "map out" physical conditions under which a piloted flame could propagate upward against a downward subsonic flow of hydrogen-air mixture in the boundary layer. In a "first-cut" simplified analysis, the potential for flashback of an "optimally-reactive" hydrogen-air mixture (near-stoichiometric) along a smooth exterior wall of the external tank was assumed to depend only on the axial velocity gradient along the boundary wall, and atmospheric pressure — both of which depend on Shuttle ascent velocity and altitude. Once these hazard potentials are identified and mapped, reduced flashback potentials involving sub-optimal mixtures would require more complex estimates of hydrogen concentrations downstream from any prescribed hydrogen vent.

The basis of this simplified flashback analysis can be found in Reference 11. Although the reported data were obtained more than a half-century ago, they appear sufficiently consistent with the authors (Pellett) relatively recent work on the extinction of non-premixed hydrogenair flames [12] to warrant their use, as described briefly below.

Figure 11, taken from Reference 11, shows the critical streamwise velocity gradient normal to a surface for flashback in various laminar flows, i.e. the gradient for flashback, laminar (gfb,L). This plot of strain-rate (or stretch-rate) limits bounds the flashback of hydrogen-air flames in cooled sub-centimeter straight tubes at 1-atm pressure, for H_2 concentrations between 10 and 78 mole percent. Note gfb,L increases from zero to a parabolic-like maximum of 11,000 1/sec at 38% H_2, and then decreases back to zero. Thus, flashback (or for that matter, ignition) cannot occur at boundary axial velocity gradients above 11,000 1/s. Furthermore, at the halfway point of 5500 1/s, flashback can only occur for mixtures between 23% and 53% H_2 (Full Width at Half Max, FWHM). Next, Figure 12, also from

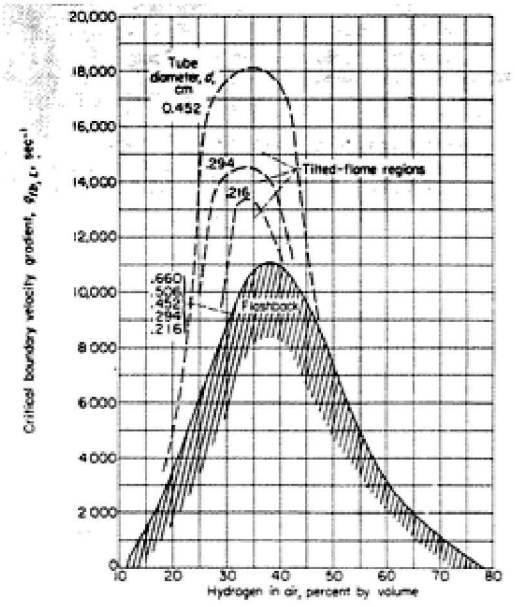

Figure 11. Critical streamwise velocity gradient normal to a surface for flashback in chosen laminar flows.

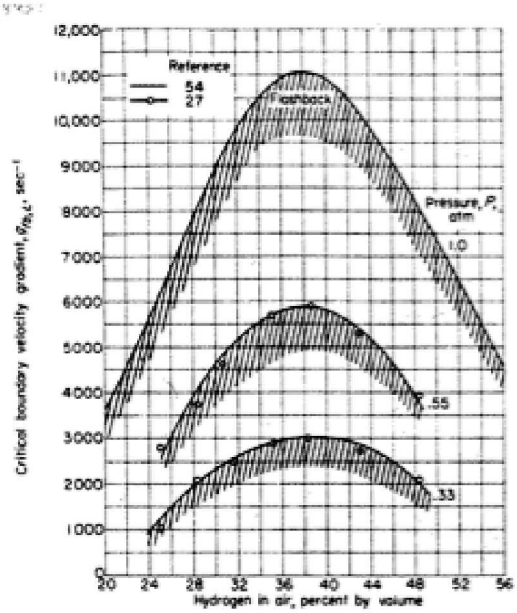

Figure 12. Effect of pressure on flashback in laminar flows.

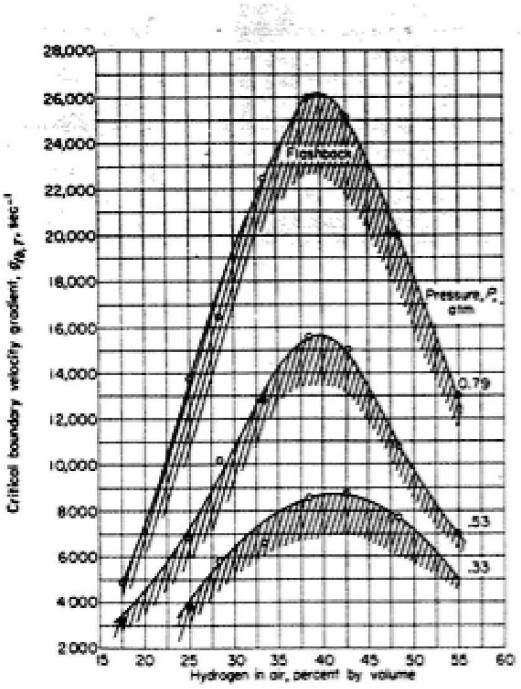

Figure 13. Effect of pressure on flashback in turbulent flows.

Reference 11, shows the effect of pressure on flashback in laminar flows, which varies as $P^{1.35}$; in the lowest pressure case (0.33 atm), gfb,L peaks at 3000 1/s for the same 38% H_2,

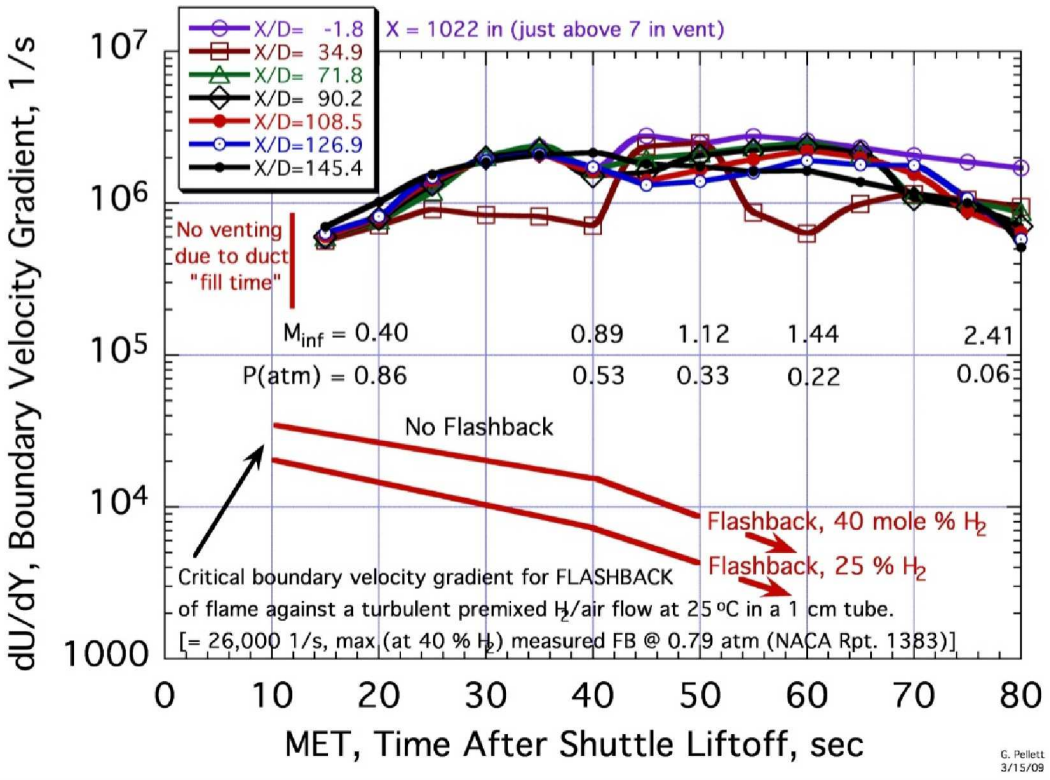

Figure 14. Boundary velocity gradient along Shuttle External Tank compared with maximum flashback potential for a piloted H_2 - air flame at $\leq$ 1 atm.

which is slightly richer than stoichiometric (29%). And finally for turbulent flows, Figure 13 shows in a similar fashion that gfb,T peaks at 26,000 1/s for 38% H_2 and 0.79 atm (with FWHM between 24% and 55% H_2), and then decreases in nearly identical fashion (as $P^{1.31}$) to 8,800 1/s at 0.33 atm.

The above-described flashback results for laminar and turbulent flows are consistent with the authors much more recent H_2 - air opposed jet burner extinction results [12], [13], [14] that are supported by 2-D numerical simulations of non-premixed H_2 - air extinction limits of Hwang [15]. Given this recent validation, the flashback potential for given boundary layer flows over a Space Shuttle external tank "smooth-surface" was assessed and mapped, once a representative set of boundary velocity gradient data were provided by Shuttle analysts. Velocity gradient data were needed at a few stations downstream from the hydrogen vent site, and at a representative set of Shuttle altitudes (speeds, and pressures), as derived from existing computed velocity profiles under (mainly) subsonic conditions.

Velocity gradient data were provided by the three-dimensional CFD calculations of the full Shuttle configuration [16]. Figure 14 is a graphical representation of all the flashback results obtained in this study using that data. Some key empirically-fitted "critical boundary velocity gradient" flashback results for turbulent flows, from Figure 13, are compared to numerically obtained boundary velocity gradient profiles along the Shuttles ET surface. The resultant streamwise boundary velocity gradients normal to the ET surface begin at an initial station one foot upstream of the D = 7 in diameter (slightly recessed) vent, followed by 6 downstream axial stations located at dimensionless distances down to X/D = 145.4, towards the bottom of the ET. The seven profiles begin at 15 sec after liftoff, where the

Mach number is 0.27 and the atmospheric pressure near the ET surface is 0.92 atm; and they extend out to 80 sec, at Mach 2.41 and 0.06 atm. Venting H_2 prior to T+15 seconds is considered catastrophic for the purposes of this study; furthermore, the CFD solutions used in this study start at T+15 seconds and increase in 5 second intervals through ascent.

The results in Figure 14 clearly show that flashback (along a smooth ET surface) is not possible by roughly a factor of 30 or more, for even the most optimum 40 mole % H_2 in air mixture, out to the limit of the (Figure 13) flashback data at 0.33 atm (50 sec). Considering the dependence of the critical boundary velocity gradient on pressure (varies as $P^{1.3}$), and our detailed knowledge of H_2 - air flame properties including extinction limits, the flashback boundary will continue to decrease out to the 80 s limit, and beyond. The flashback limit shown for a sub-optimal mixture of 25 % H_2 gives a similar picture, but the 30 x "factor of safety" expands to roughly a factor of 50. It can be seen in Figures 13 and 14 that lower H_2 concentrations will continue to widen the gap between flashback and expected boundary velocity gradients along the smooth ET surface. Obviously, the large and widening factor of safety helps mitigate the possibility of localized flameholding in the vicinity of significant surface bumps and obstructions, that might otherwise help stabilize a wake flame by virtue of flow recirculation.

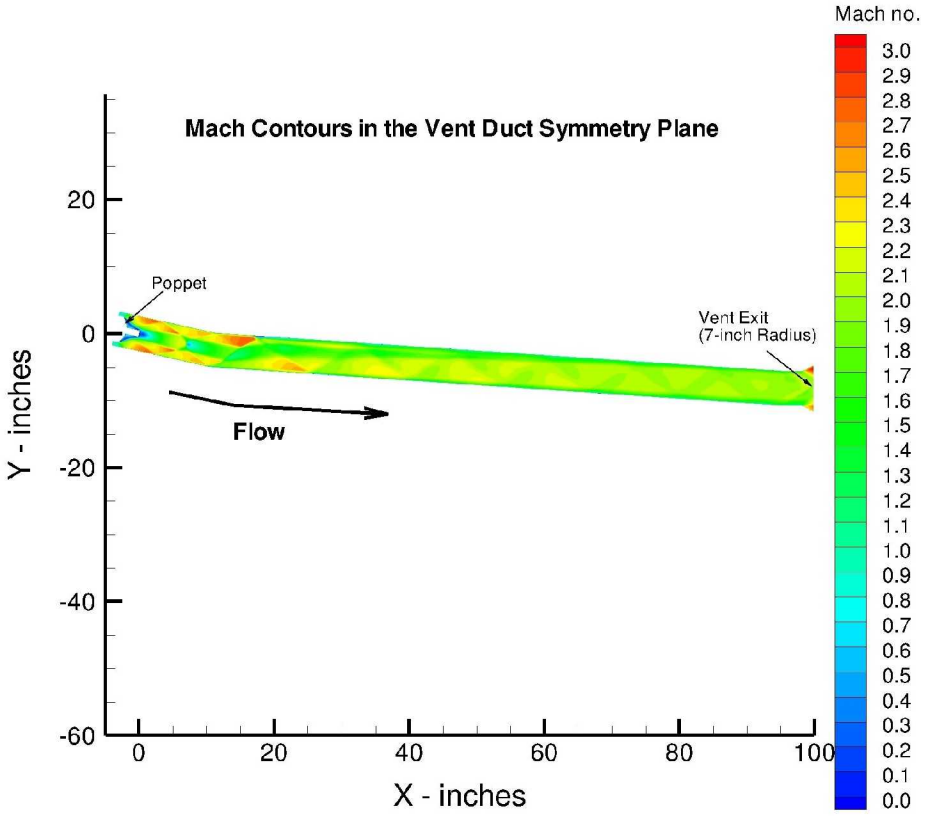

Figure 15. Mach contours in the symmetry plane showing the flow along the length of the vent duct.

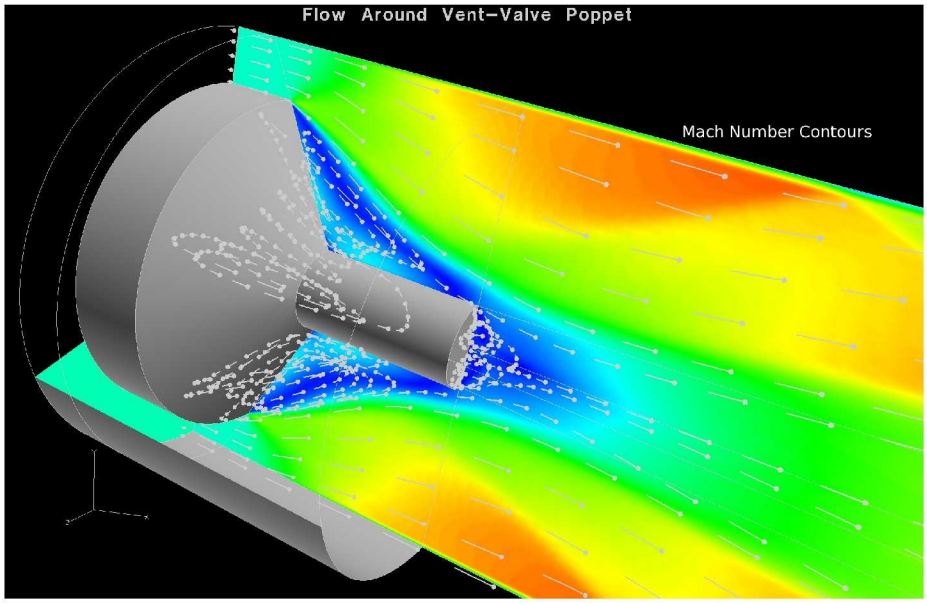

Figure 16. Flow around the poppet head, Mach Contours and streamline filaments.

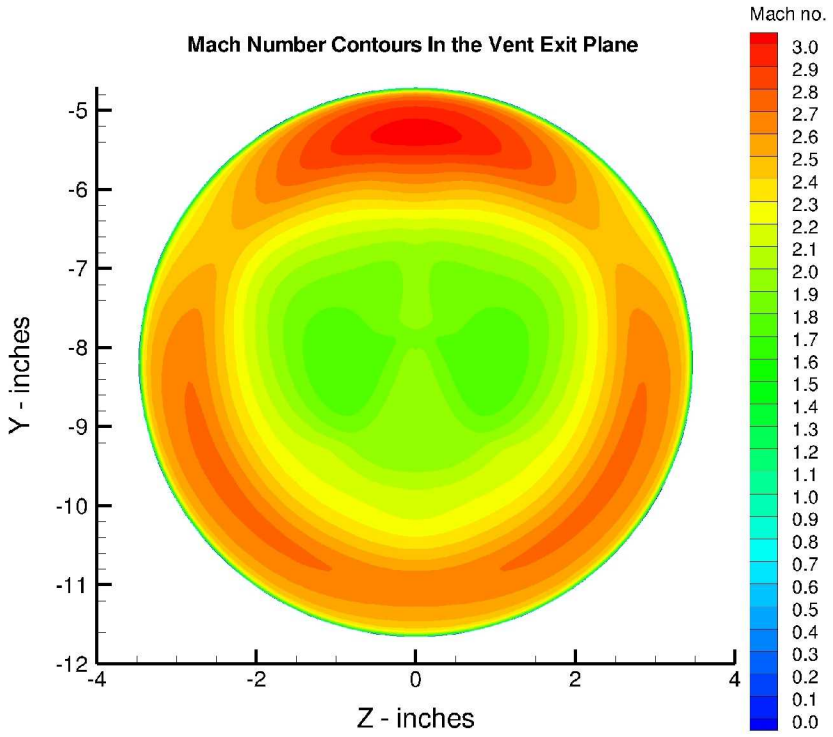

Figure 17. Mach contours in the plane of the 7-inch vent exit.

3.4 Shuttle Vent Calculations

The final section of the external tank pressure relief system consists of a 5.125 inch diameter duct with a poppet valve at the upstream end and an expansion to a 7 inch diameter outflow

at the surface of the tank. There are two turns in the duct, with the first turn 8.78 degrees and the second 3.88 degrees. Vent pipe conditions provided for the study [17] were based on ullage pressures and temperatures at selected points in the flight trajectory and a vent spillage area of 8.684 in^2. This flow area was determined to be the maximum area that would occur from a poppet failure. At an MET of 55 seconds, the properties were extracted from a table [16]. The mass flow rate was 2.387 lb_m/second, the total temperature 220.65 K and velocity was assumed to be sonic around the poppet head. At the start of the analysis, pressure losses through the vent duct were not known. Two different sets of vent exit conditions were computed based on 1) isentropic expansion from the poppet valve to the vent exit, 2) pressure losses leading to choked flow at the end of the 5 inch duct section followed by an isentropic expansion to the 7 inch exit diameter. The first method lead to an exit Mach number of 3.11 which seemed excessive. The second method lead to an exit Mach number of 2.14. Since the jet exit conditions determine the amount of penetration of the hydrogen jet into the flow around the ET, a calculation using 3-D CFD was done to provide a better estimate of the vent exit conditions. Figure 15 shows Mach numbers in the symmetry plane along the length of the duct. Shockwaves and expansion waves can be seen along the length of the duct.

The VULCAN (Viscous Upwind aLgorithm for Complex flow ANalysis) code [20] was used for the calculation. The 2.9 million point grid was generated with the GRIDGEN code with the assumption of a flow area of 8.684 in^2 around the poppet. The geometry was assumed to be symmetric from side to side. Figure 16 shows the poppet head with Mach number contours in the symmetry plane and streamline filaments in separated regions near the surface of the poppet. The sonic flow expands around the poppet and creates a series of shockwaves and expansion fans which propagate down the duct.

Figure 17 shows Mach number contours in the plane of the 7-inch diameter vent exit. The higher Mach numbers around the perimeter of the exit are due to the expansion waves generated at the transition from the 5-inch to the 7-inch duct sections. A one-dimensionalization of the exit flow using the conserved-flux approach yields an averaged exit Mach number of 1.93, a static temperature of 121.94 K and a static pressure of 13.73 kPa. This exit Mach number is slightly lower than the 2.14 computed assuming the flow is choked at the end of the Mach 5 duct section, however, there is some variation in the exit Mach number depending on the method used to average the exit flow. In fact a mass-flux-weighted method of the same exit plane results in an averaged exit Mach number of 2.15. As a result, the mixing studies done with the Mach 2.14 exit properties were considered to be very reasonable.

3.5 Three-Dimensional Simulations

The final step in the analysis of the Shuttle hydrogen venting problem utilizes three-dimensional computational fluid dynamic (CFD) modeling of the flow field about the external tank near and downstream of the hydrogen vent. The physics of this flow field requires that the problem be analyzed with consideration of the turbulent air flow that is present on the Shuttle external tank, the turbulent mixing of the gaseous hydrogen that is released into the air flow, and the possible occurrence of finite-rate, multi-component chemical reaction of the mixture. A final calculation might also consider the coupled effect of the turbulence on chemical reaction and the effect of the chemical reaction on the turbulence field. This final calculation would carry the study of this problem to the state-of-the art limit of CFD for turbulent high-speed chemically reacting flows.

A series of CFD calculations was proposed that start with a simplified geometry and reduced physics and subsequently, as experience is gained with results from each simulation, the analysis increased as necessary in complexity of geometry and physics [3]. Additionally, calculations were initiated at one trajectory point, and augmented with other trajectories as determined by prior results.

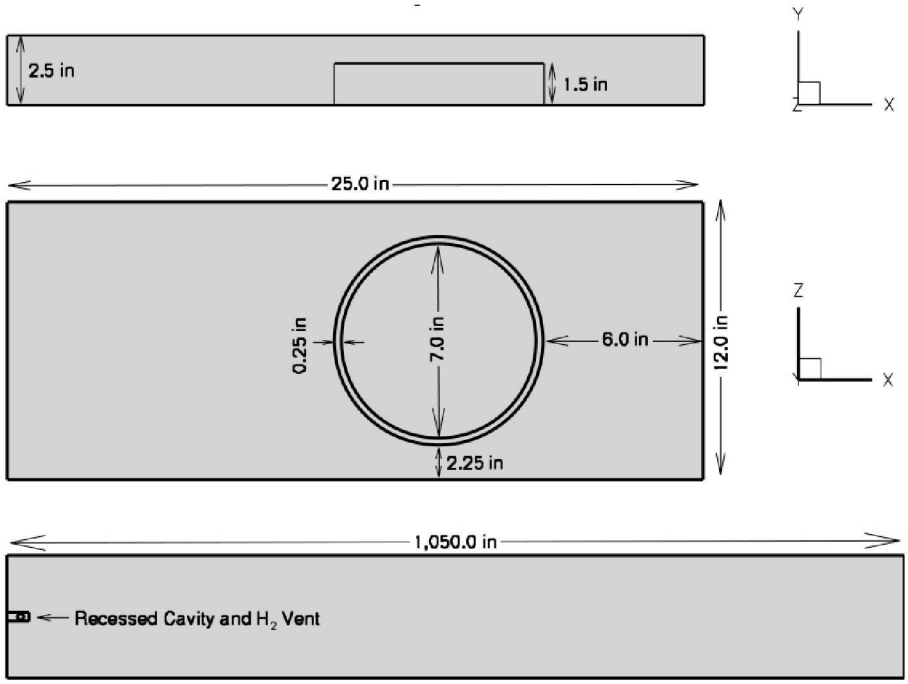

Figure 18. Configuration of H_2 vent and surrounding cavity.

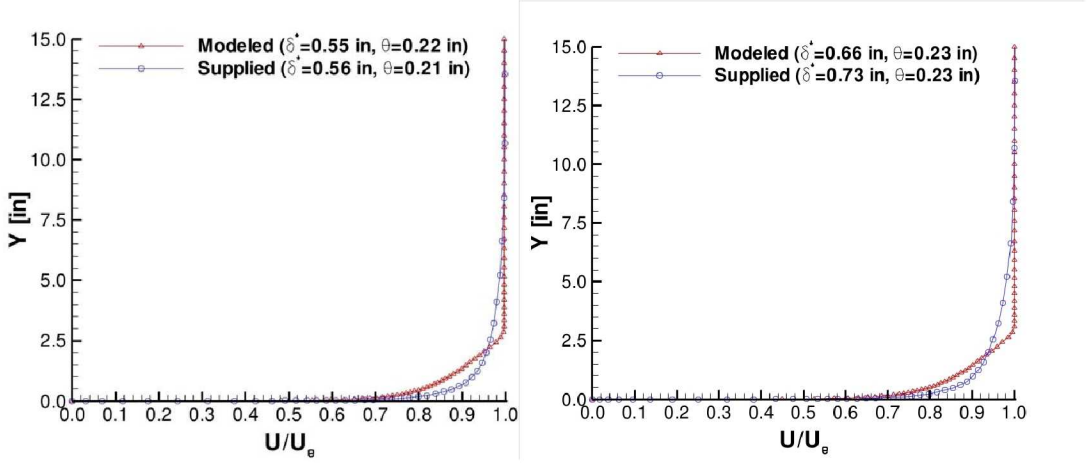

MET = 55 seconds MET = 75 seconds

Figure 19. Comparison of approach external tank velocity profiles just upstream of the vent.

The first series of calculations that was proposed considered a flat plate with normal flush-wall hydrogen injection with a cavity sized to match the one that houses the hydrogen vent on the external tank. This series of calculations ignores the curvature of the external tank and any intervening flow structure (rib structure, structural projections, etc.). The proposed calculations include the following steps:

1. Model a non-reacting flow to evaluate the species mixing and determine the axial

MET	M	T(K)	P(kPa)
55	1.68	197.44	16.758
75	1.92	222.22	9.4563

Table 2. Boundary layer edge conditions.

MET	M	T(K)	P(kPa)
55	2.14	111.18	12.577
75	2.20	109.26	10.617

Table 3. Vent edge conditions.

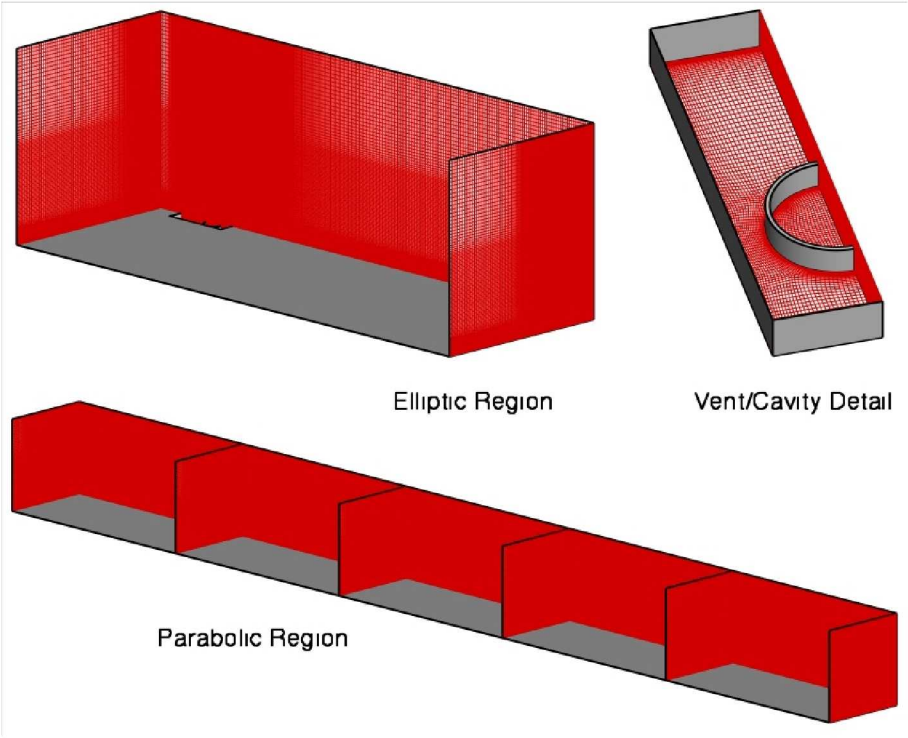

Figure 20. Grid generated for the hydrogen/air vent mixing study.

location where the concentration of hydrogen drops below the flammability limit (if at all).

2. Repeat the above study with the inclusion of finite rate kinetics for hydrogen and air. This study will also involve the inclusion of local hot spots to act as ignition sources to determine the critical regions that could lead to flameholding and subsequent flame propagation.

To date, the calculations required for step (1) above have been completed.

The flat plate geometry considered is shown in Figure 18. The plate length of 1050 in was chosen to match the length measured from the vent location to the exit of the external

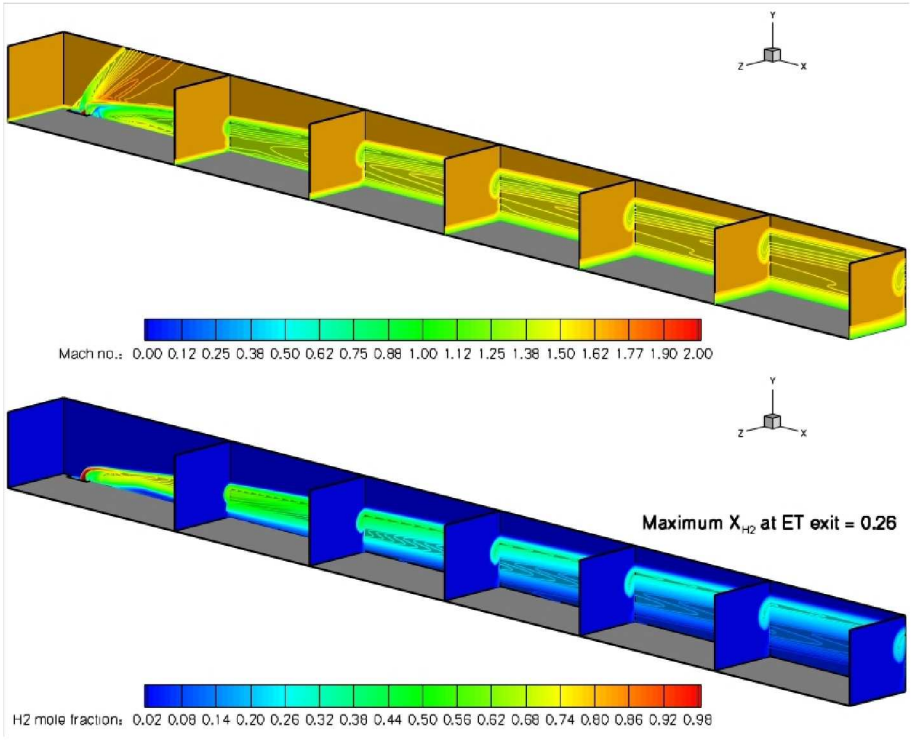

Figure 21. Mach contours and hydrogen mole fraction contours at MET = 55 seconds.

tank. This length corresponds to roughly 145 vent diameters. The half-width of the plate (spanwise or z-length) and the wall-normal extent were both chosen as 70 inches (10 vent diameters). These dimensions were chosen based on estimates of the plume spreading rate along the length of the plate. The desire was to have the computational domain contain the entire extent of the hydrogen plume as it convects and diffuses downstream.

The freestream conditions that were considered were the conditions that corresponded to the MET=55 seconds and MET=75 seconds trajectory points. Existing CFD solutions for the flow over the external tank at these trajectory points were provided to the Langley analysis team [16]. The local flow properties just upstream of the vent location were extracted from these solutions to provide the external tank boundary layer information to be matched by the flat plate analysis. A comparison of the supplied boundary layer profiles and the flat plate profiles with matched displacement and momentum thickness are shown in Figure 19. The boundary layer edge conditions for the MET = 55 and 75 second trajectory points are given in Table 2.

The hydrogen vent conditions were based on estimates provided for the maximum vent flow rate at each of the trajectory points. The maximum vent flow rate at the MET = 55 second trajectory point was 1.18 kg/s at a total temperature of 220.65 K. The maximum vent flow rate at the MET = 75 second trajectory point was 1.03 kg/s at a total temperature of 223.15 K. The vent conditions at the exit of the 7-inch diameter vent duct were computed based on an assumption that the flow would become choked at the exit of the 5-inch diameter piping just prior to expansion to the 7-inch duct diameter. The expansion from the 5-inch to the 7-inch diameter section was assumed to take place isentropically. This assumption was supported by an additional CFD analysis that was performed for the internal vent piping at the MET = 55 second condition as given in Section 3.4. The resulting vent exit conditions

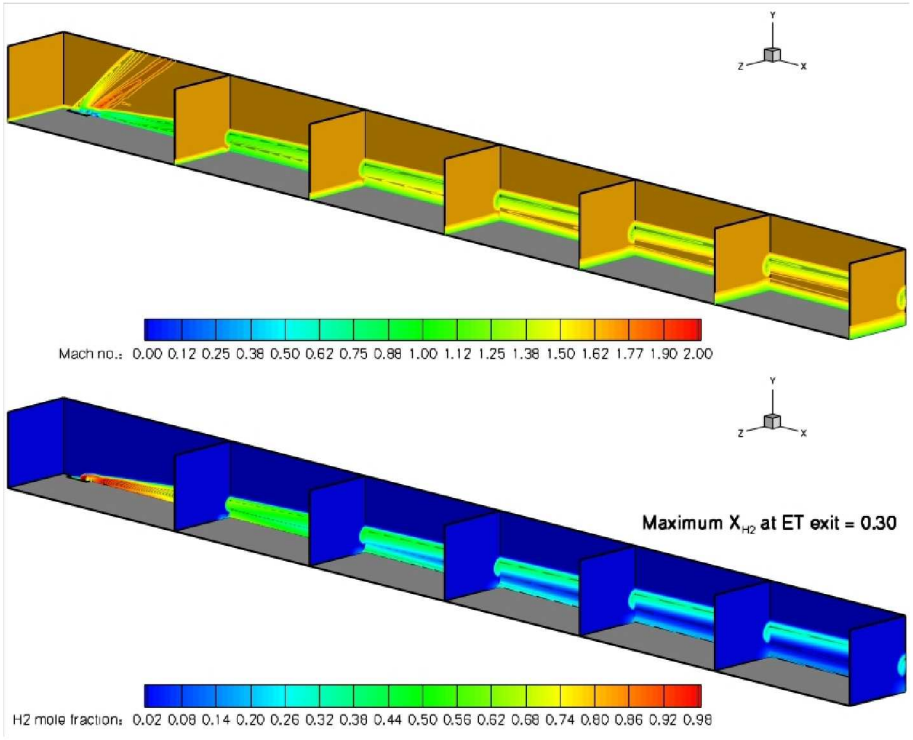

Figure 22. Mach contours and hydrogen mole fraction contours at MET = 55 seconds (reduced vent flow rate).

are given in Table 3.

All of the CFD results were obtained using the VULCAN Navier-Stokes code. The code solves the unsteady, Reynolds-averaged conservation equations appropriate for calorically or thermally perfect gases with a cell-centered finite volume scheme. Efficient utilization of parallel architectures is realized through calls to MPI (Message Passing Interface) routine using an SPMD (Single Program Multiple Data) paradigm, a natural choice for multi-block flow solvers. A variety of upwind formulations are available for evaluating the inviscid fluxes, while central differences are used for the viscous fluxes. The software supports both implicit and explicit time integration strategies for either steady-state or unsteady simulations. A variety of one-equation and two-equation turbulence models are available to describe turbulent flows, and chemical reactions are accounted for with finite rate kinetics or a mixing controlled model based on eddy break-up concepts. Further details describing the code are found in Reference 20.

The grid generated for the flat plate mixing analysis is shown in Figure 20. This grid consists of roughly 24 million cells. The hydrogen vent cross-section plane was resolved with 1024 cells. The grid was clustered to all solid surfaces at a level suitable for the use of wall functions, i.e. y^+ values for the first cell center away from the wall were on the order of 25. The maximum grid spacing in the streamwise direction was 0.5 inches (1/14 of the vent diameter). This grid spacing limitation was also maintained in the spanwise and wall-normal directions in all regions expected to contain vented hydrogen. To expedite the computations, the computational domain was broken up into two distinct regions. The upstream region, which contained the vent and cavity housing was solved using a full elliptic algorithm. The downstream region contained fully supersonic flow outside of the boundary

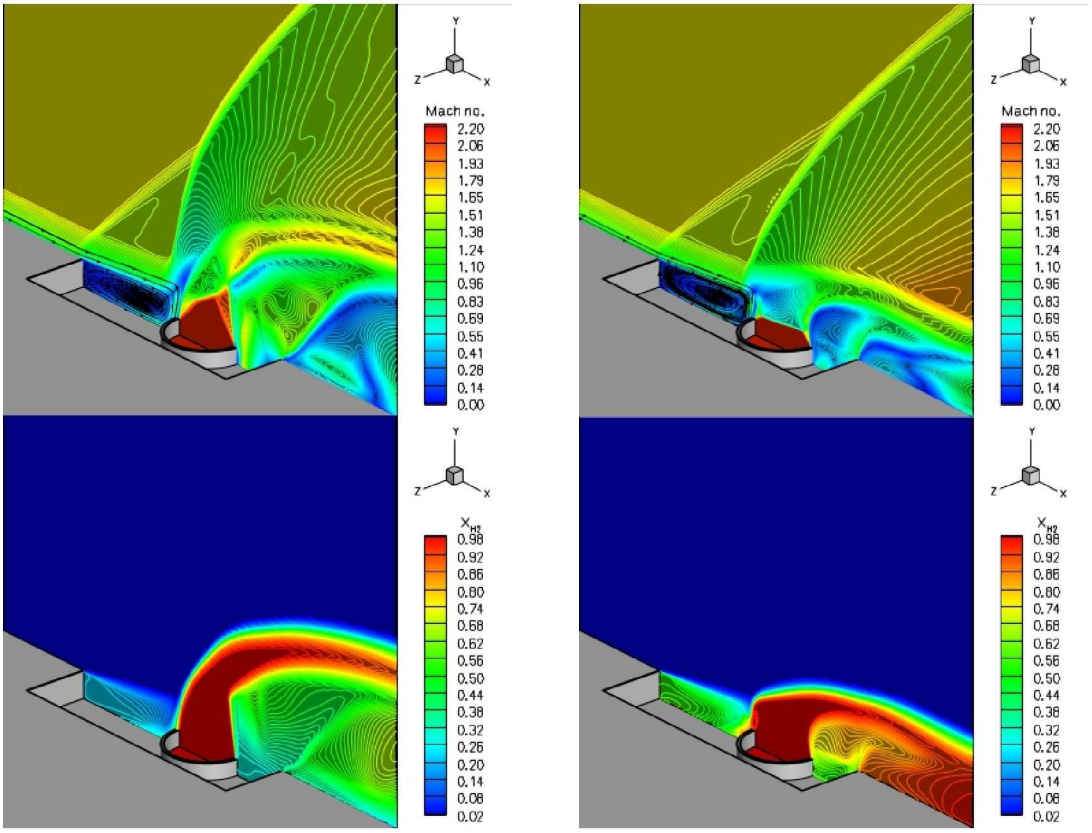

Maximum vent rate Reduced vent rate

Figure 23. Mach contours and hydrogen mole fraction contours at MET = 55 seconds in the vicinity of the vent.

layer, so this section was solved using a more cost-effective parabolized algorithm.

Figure 21 shows the Mach contours and hydrogen mole fraction distribution along the full length of the computational domain at the MET = 55 second trajectory point. At this vent condition (which was the maximum expected vent flow rate), the vented hydrogen plume has completely penetrated through the boundary layer. The counter-rotating vortex pair created by the injection of hydrogen into the supersonic external flow has lifted the hydrogen plume well above the boundary layer of the external tank. Hydrogen levels at the exit plane inside of the plume are at nearly stoichiometric proportions. Hence, a flammable mixture is still present at the exit of the external tank at this vent condition. Note that there are no appreciable levels of hydrogen in the external tank boundary layer. However, there are substantial differences in external flow structure of the shuttle (e.g. shocks off of the solid rocket boosters, tank curvature effects, etc.) as compared with this flat plate simulation. Hence, one should not draw too many conclusions about the positioning of the hydrogen plumes based solely on the present flat plate study.

The penetration of the vented hydrogen through the external tank boundary layer prompted the consideration of an additional simulation with a reduced vent flow rate. The reduced flow rate was arbitrarily chosen as half of the maximum flow rate condition, which results in a pressure at the vent exit that is half of the value employed at the maximum vent mass flow condition. The results of this simulation are shown in Fig 22. This condition also showed the vented hydrogen to penetrate through the boundary layer, but not to the

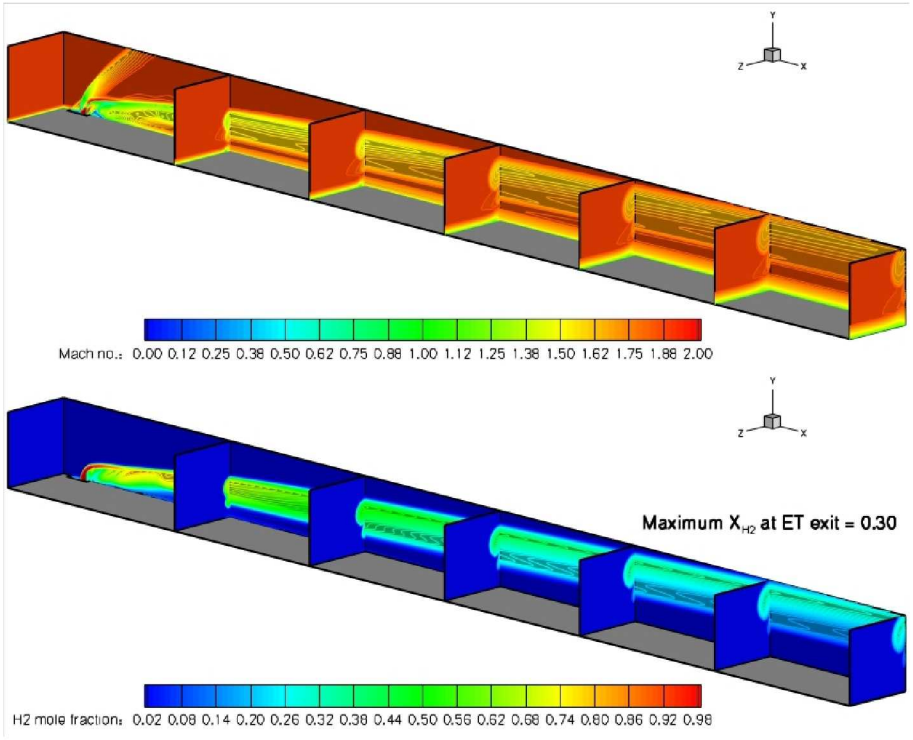

Figure 24. Mach contours and hydrogen mole fraction contours at MET = 75 seconds.

extent seen with the maximum flow rate condition. In fact, there are substantial levels of hydrogen still present in the boundary layer at the exit of the domain, which poses a higher risk for combustion due to the higher temperatures that would be present in the boundary layer.

Figure 23 shows a detailed view of the flow structure in the vicinity of the vent. A complex array of shock waves and expansion fans are clearly visible as the vented hydrogen adjusts to the surrounding supersonic cross flow. These structures include a separation shock (which is attached at the cavity leading edge) and a barrel shock, both of which are typical of high momentum flux ratio injection into a supersonic stream. Another particularly noteworthy feature is the comparison of the hydrogen levels inside of the cavity. The maximum vent rate shows the cavity to be primarily in a fuel lean state due to the rapid penetration of the hydrogen through the boundary layer. The lower vent rate simulation contains both fuel rich and fuel lean conditions within the cavity and may pose a larger flameholding risk than the maximum vent condition.

Figures 24 (maximum vent condition) and 25 (reduced vent condition) show the Mach contours and hydrogen mole fraction distribution along the full length of the computational domain at the MET=75 second trajectory point. As was the case with the MET=55 second simulations, the vented hydrogen plume has completely penetrated through the boundary layer. The results obtained at the maximum vent flow rate show no appreciable levels of hydrogen in the boundary layer, but once again the reduced vent rate shows the presence of a combustible mixture inside the boundary layer at the exit of the external tank. Figure 26 shows a detailed view of the flow structure in the vicinity of the vent at the MET=75 second condition. The same flow structures described previously are also present at this flight condition, and once again, the reduced vent rate condition poses the highest risk of

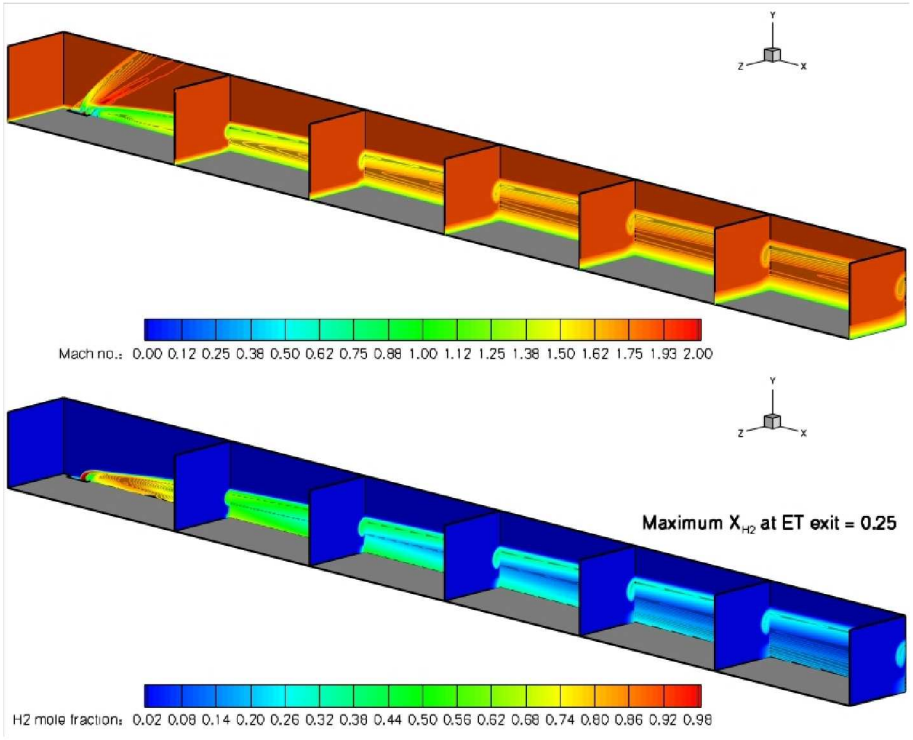

Figure 25. Mach contours and hydrogen mole fraction contours at MET = 75 seconds (reduced vent flow rate).

flameholding based on the fuel to air ratio comparisons inside the cavity.

Following completion of the three-dimensional analyses, a comparison was made between the JetPen results of Section 3.2 and the VULCAN 3-D results. Figure 27 shows the comparison between the VULCAN and JetPen results for the full and half mass flow simulations performed with the 5-inch choked jet conditions. For the VULCAN results, the bulk flow was defined as the average concentration of hydrogen contained in the plume area at a given axial location. The plume area is defined as the region where the hydrogen concentration is greater than 0.001 of the maximum hydrogen concentration at that axial location. An equivalent plume diameter was calculated from this area and was similar to that calculated by JetPen. The results show a good agreement between the JetPen and VULCAN code in regions away from the jet exit with both sets of results showing a combustable hydrogen mixture reaching to the end of the tank.

4 Confidence Levels of Approach and Analysis

The conclusions drawn in this paper regarding the Shuttle gaseous hydrogen venting risk from flow control valve failure are based on empirical modeling or numerical simulation with the exception of the flashback analysis which also utilizes experimental data. Therefore, confidence levels for the conclusions drawn must be determined by assessing the potential sources of error inherent in the experimental data and the empirical and numerical tools that were utilized.

The jet mixing analysis utilizes an empirical model for the actual hydrogen release mechanism to predict the spread of an impinging jet into a cross-flow. The model and the code

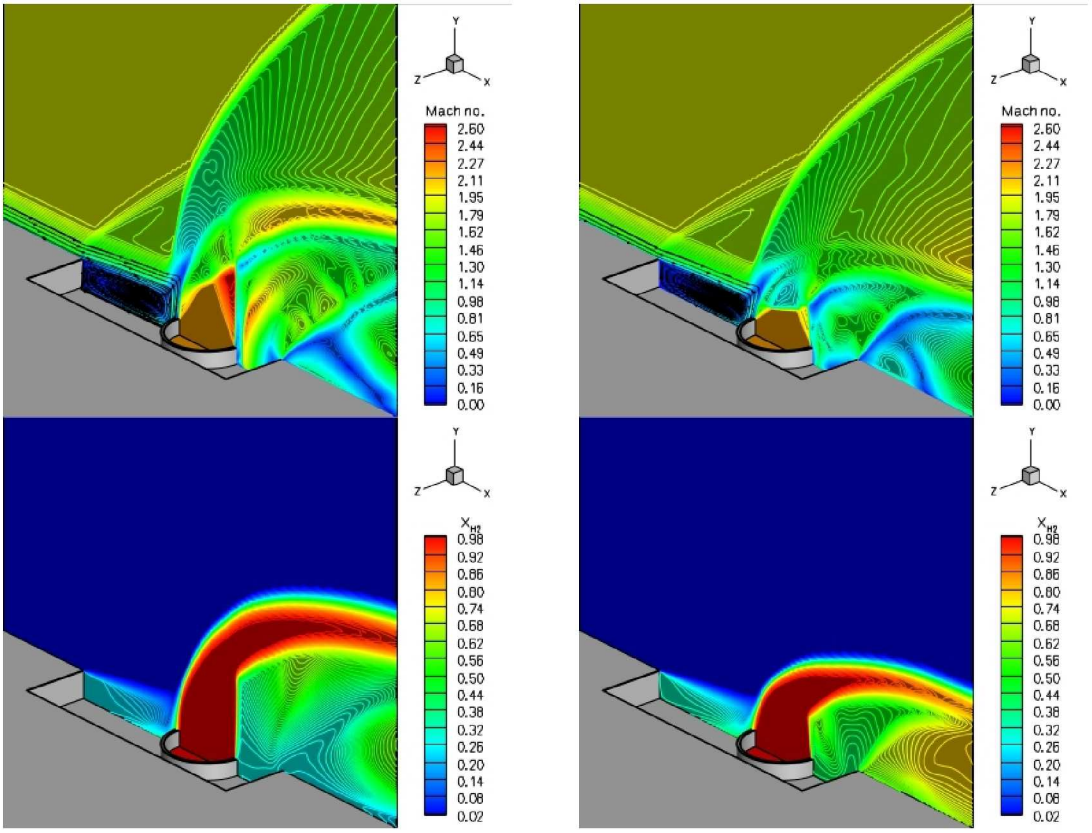

Maximum vent rate Reduced vent rate

Figure 26. Mach contours and hydrogen mole fraction contours at MET = 75 seconds in the vicinity of the vent.

utilizing the model, JETPEN, are based on the similarity between a jet discharging into a quiescent medium and a jet discharging into a cross-flow. Correlations allow the calculation of the complete trajectory of the jet as well as the properties of the jet such as bulk H_2 mass concentration. Results utilizing the correlations are compared with data in Reference 6 and give reasonable agreement. Therefore, the source of error when utilizing the correlations for the Shuttle analysis is the effect of differences in the Shuttle environment as compared to the conditions under which the correlations were developed.

The data utilized in the flashback analysis were taken from a well accepted source [11] that had been utilized in similar previous studies. The data, while old, was validated by more current experimental data [12], [13], [14] and simulations [15]. Therefore, it seems reasonable to accept this data to define the probability of flashback in a hydrogen - air mixture. It must be remembered, however, that the decision regarding flashback made using Figures 11, 12 and 13 from Reference 11 requires velocity gradient data that are taken from numerical simulations. Therefore, flashback analyses are only as reliable as the gradient information derived from these simulations.

Numerical simulations rely on varying degrees of empirical information or phenomenological modeling. Both the well stirred reactor analysis and the three-dimensional simulations required accurate hydrogen - air kinetics mechanisms and finite rate kinetics models to yield accurate chemical species predictions as a function of temperature, pressure and species present in the initial fuel-air mixture. Hydrogen - air kinetics mechanisms are reasonably well

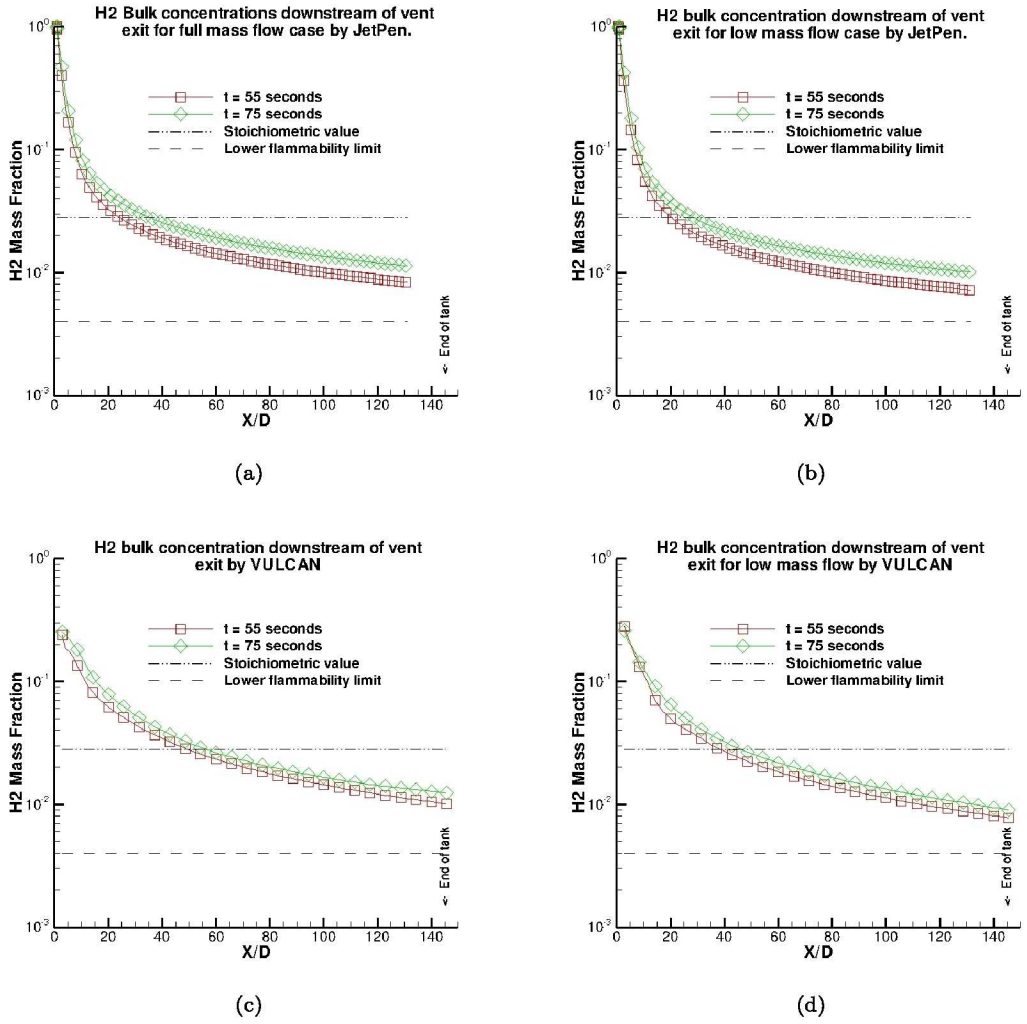

Figure 27. Comparison of JetPen with VULCAN simulations.

known compared to mechanisms for other fuels and it is felt that recent models, that account for both the effects of temperature and pressure, provide a reasonably accurate representation of reaction physics. The finite rate models derived from these mechanisms introduce additional error as the models fit experimentally derived chemical behavior to empirical models representing the chemistry. Hydrogen - air chemistry is a *relatively* straightforward system compared to other fuel-air systems, e.g. hydrocarbons, and hydrogen - air systems have been studied by many researchers over many years. The models utilized in this study have a high degree of certainty within their range of applicability. The principle exception to this statement may be the lower range of pressures over which the models are used in this study. However, technical discussions with subject matter experts in this area [18] suggest that the applicability of current models are likely to be valid at pressures that are below those used to develop the kinetic mechanisms. The rationale with this assertion is a result of the fact that these mechanisms have been validated with pressures that are within the "lower pressure limit" of hydrogen - air kinetics. In this limit, the pressure dependence on the kinetics is linear, hence the models are expected to perform reasonably well when

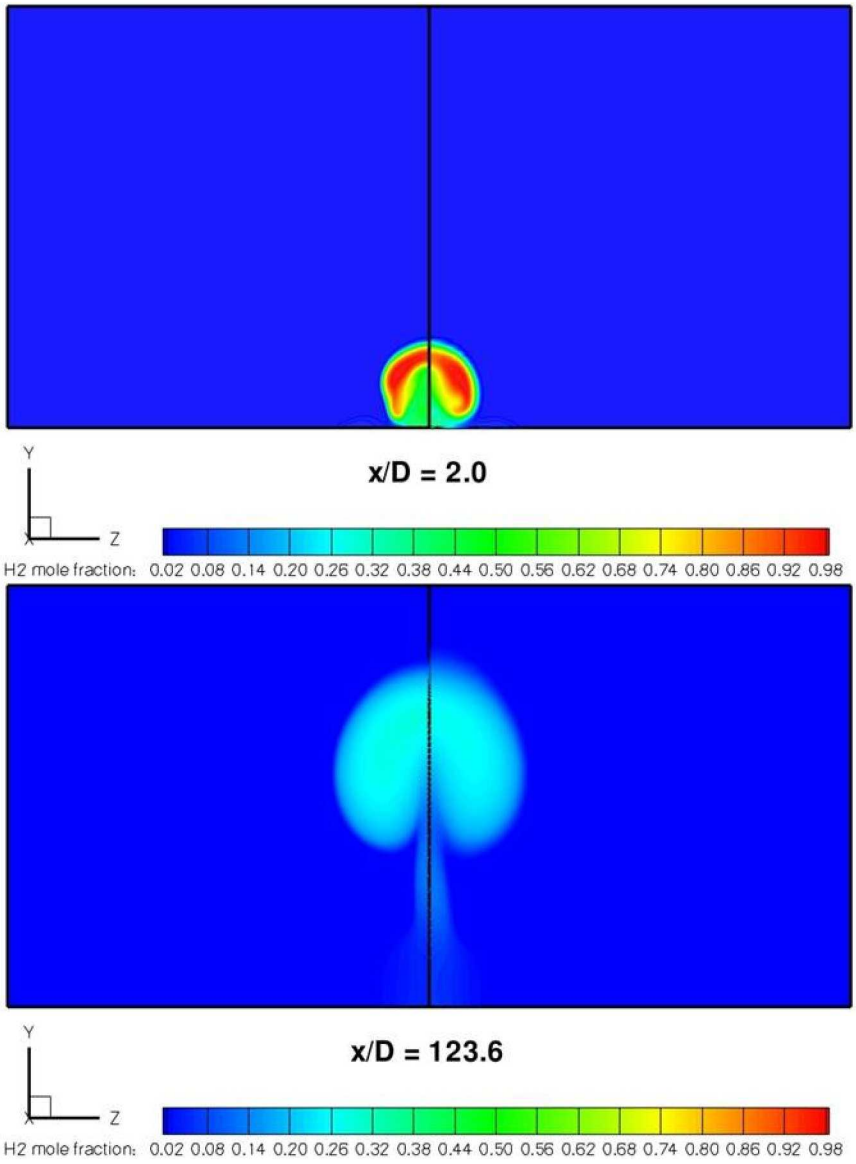

Figure 28. Sensitivity of the vented hydrogen mole fraction distribution to grid density (fine grid - left of symmetry line, coarse grid - right of symmetry line).

extrapolated to pressures below this limit.

The three-dimensional numerical simulation tools utilized in the current study require the most scrutiny when assessing confidence levels of the overall analysis. These tools solve highly nonlinear complex partial differential equations to describe turbulent, chemically reacting high-speed flow. When turbulent fluctuations and chemistry are introduced into the governing equations utilizing Reynolds and Favre averaging [19], terms appear that cannot be "closed," i.e. the terms cannot be mathematically described in an exact manner. Empirical relationships or phenomenological models, i.e. models *representing* the actual physics, must then be introduced. The phenomenological models for the turbulence, chem-

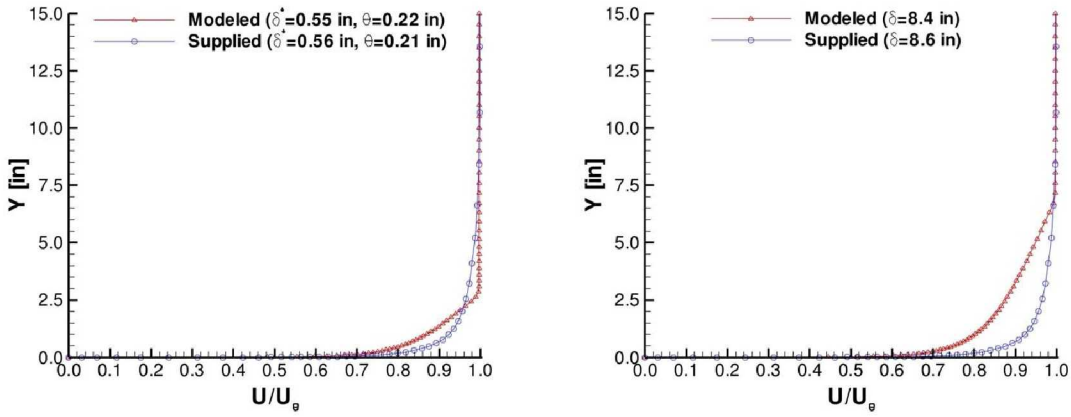

Matched displacement and momentum thickness

Matched boundary layer thickness

Figure 29. Comparison of supplied and flat plate external tank boundary layer profiles.

ical species transport and reaction, and the interaction between turbulence and chemical reaction introduce varying degrees of error depending on how well the models represent the physical flow. These errors are difficult to assess since they are created by failure of the models to completely represent the individual contributions to the physics within the coupled highly nonlinear behavior of the fluid physics and its governing equations. Assessment of overall error is therefore best made by comparing results from the codes to data from a series of experiments representing increasing complexity while approaching the current problem under study. The VULCAN code utilized in this study has undergone this test for a number of internal flow configurations with combustion and for some external configurations. A number of examples are given in Reference 20. Shuttle external flows over the range of conditions encountered in flight have not been studied, but a subset of external flow problems encompassing part of the Shuttle flight envelope on simpler geometries have been considered.

The most critical element of the current simulations with respect to modeling is the representation of the turbulence field. The turbulence models that are utilized have in general been developed for turbulent flows on flat plates. The release of a transverse jet of hydrogen into the flow field introduces additional complexities including flow around the jet, a gas mixture, regions of separated flow around the hydrogen jet and the potential for chemical reaction with attendant heat release. In the current analysis, turbulent mixing of the fuel and air is described using a turbulent Schmidt number that is assumed by experience. By assuming a reasonable range of Schmidt numbers, the range of mixing can be bracketed within a range of expected distributions. The turbulent diffusion of the heat released due to chemical reaction is controlled by the assumed value of the turbulent Prandtl number. The values are again chosen by experience, resulting in the same sources of uncertainty described for the Schmidt number.

Discretization errors can also contribute to solution degradation. Discretization errors result from the failure of the discretized form of the governing equations, i.e. the numerical representation of the partial differential equations, to properly represent the actual governing equations system. This error can be evaluated and then minimized by solving a given problem on several computational grids of increasing size (and decreased grid spacing) on a fixed domain and then projecting the degree of error using extrapolation. Based on this error estimate, an appropriately sized computational grid can then be chosen for a desired degree of error. Therefore, discretization error can be minimized to an acceptable degree

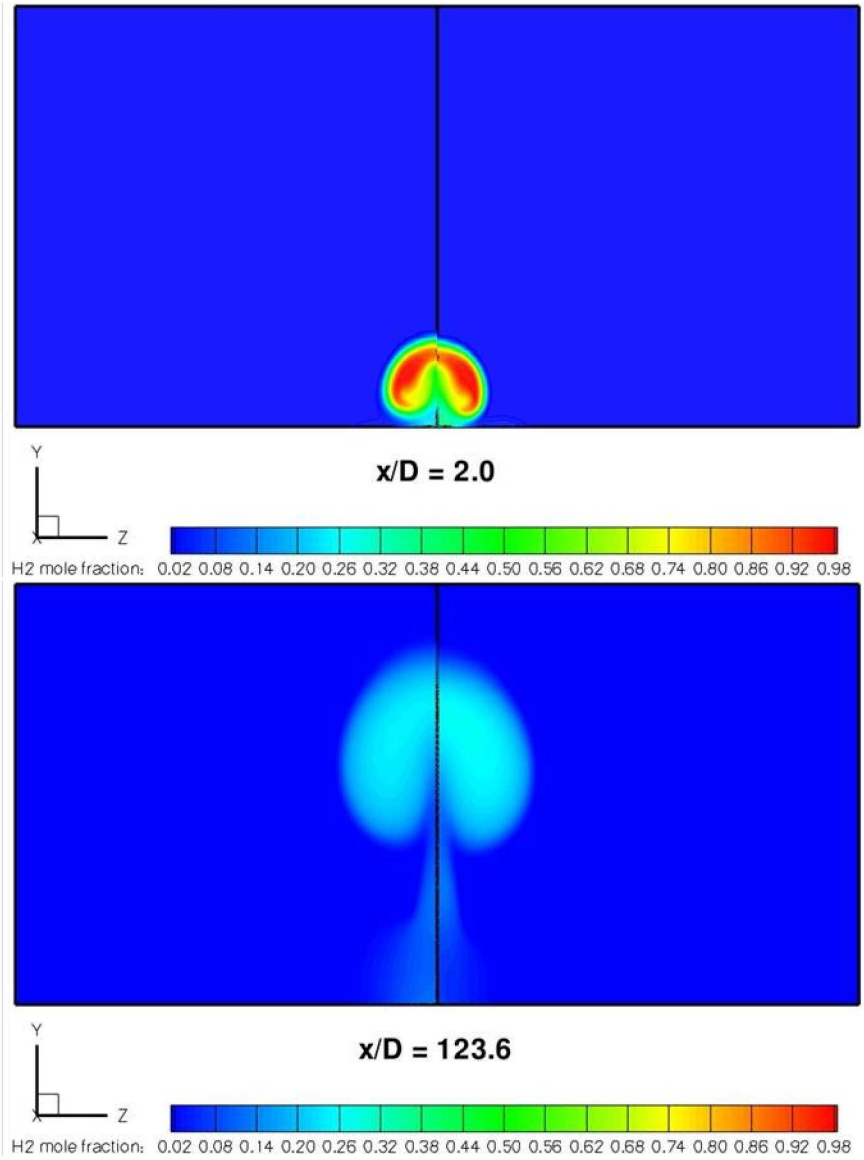

Figure 30. Sensitivity of the vented hydrogen mole fraction distribution to assumed approach external tank boundary layer (matched raw thicknesses - left of symmetry line, matched integral thickness - right of symmetry line).

within the constraint of computer resources.

Other sources of uncertainty are related to the supplied boundary conditions themselves. There are a multitude of failure modes that can lead to hydrogen venting, and only a small subset can be analyzed within a reasonable time frame. Hence, some assessment should be performed to determine the sensitivity of the solution to various vent conditions. Similarly, it is not possible to match all aspects of the approach boundary layer supplied to the Langley research team with that formed by an equivalent freestream flow over a flat plate. This uncertainty requires that additional simulations be performed to assess the importance of

the approach boundary layer as it relates to the hydrogen/air mixing processes.

An effort was taken to try to understand the sensitivities involved with each of the uncertainties that have been described above. In particular, the following sensitivities were assessed:

1. Sensitivity to discretization error
2. Sensitivity to the external tank boundary layer profile upstream of the vent
3. Sensitivity to turbulence model
4. Sensitivity to turbulence scalar mixing model (turbulent Schmidt number)
5. Sensitivity to vent condition

All of these sensitivities were performed at the MET=55 second trajectory point.

The effect of discretization error is considered first. To assess the adequacy of the grid employed, a coarsened version of the existing grid was formed by removing every other grid point in all three coordinate directions. This results in a grid with 1/8 of the cell count (roughly 3 million cells) of the original 24 million cell grid. Hydrogen mole fraction distributions are compared at two axial stations downstream of the vent. The first station is in the vent nearfield (x/D = 2) and the second station was near the exit of the external tank (x/D = 123.6). Figure 28 shows the comparison of hydrogen mole fraction for each grid system. In each of these images, the image on the left half of the symmetry line is the fine grid result, while the image on the right half of the symmetry line is the coarse grid result. At an x/D of 2.0, there are some slight differences noted in the structure of the fuel plume. However, the overall plume shape and penetration level is well predicted on both grid systems. Similarly at the station far downstream (x/D = 123.6), both grid systems show a similar level of penetration and plume structure shape. The coarse grid does show the plume to have mixed out slightly more rapidly than the fine grid result, but this trend is to be expected with the added numerical dissipation associated with the use of a coarser grid. The important conclusion to draw from these images is that both grid systems have resolved the same salient flow physics, suggesting that the discretization errors are not excessive. Based on the favorable level of agreement between the coarse and fine grid results, the remainder of the sensitivity studies have been performed using the coarse grid.

The effect of the state of the external approach boundary layer is considered next. The boundary layer parameters that were matched between the supplied boundary layer profile and the equivalent flat plate profile were displacement thickness and momentum thickness. However, as evident in Figure 29, the raw boundary layer thicknesses are not well matched. Hence, an additional simulation was performed using an approach boundary layer that matched the raw thickness of the supplied velocity profile. The comparison of this profile with the supplied boundary layer profile is also shown in Figure 29. The effect that the assumed boundary layer state has on the penetration and spread of the vented hydrogen plume is shown in Figure 30. The plume penetrates somewhat further into the freestream flow when the larger boundary layer thickness is assumed upstream of the vent, due to the larger momentum deficit of the approach flow. However, the differences in the evolution of the fuel plume are minimal. Hence, the uncertainty associated with the assumed approach boundary layer condition is not expected to influence any of the conclusions that have been drawn for the CFD results that have been presented.

The sensitivity of the solution to the modeled levels of scalar diffusion are considered next. The turbulent Schmidt number scales the rate of turbulent species diffusion relative to turbulent diffusion of momentum. Smaller values of the Schmidt number will correspond to enhanced levels of species diffusion. There are no absolute bounds available for the

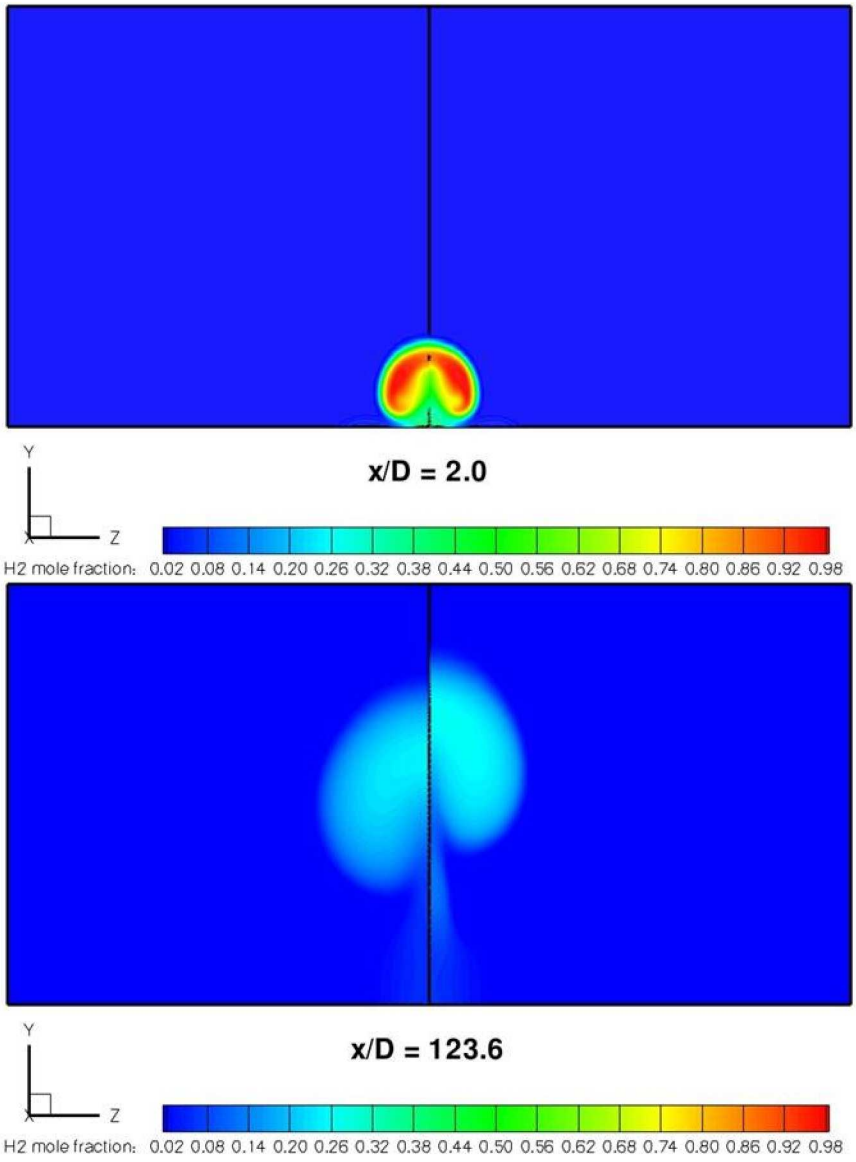

Figure 31. Sensitivity of the vented hydrogen mole fraction distribution to choice of turbulence model (Menter model - left of symmetry line, Wilcox model - right of symmetry line).

turbulent Schmidt number, but experience has shown that values between 0.25 and 1.0 tend to collapse simulation results to available experimental data. A value of 0.5 was used in the results discussed previously, so two additional simulations were performed with half (0.25) and twice (1.0) this default value. The results of these simulations are shown in Figure 32. At the x/D=2.0 station, the results obtained for both bounding limits of the turbulent Schmidt number are similar, although the plume predicted from the turbulent Schmidt number of 0.25 simulation has diffused to a greater extent. As the plume mixing becomes more diffusion dominated, the influence of the Schmidt number is even more apparent.

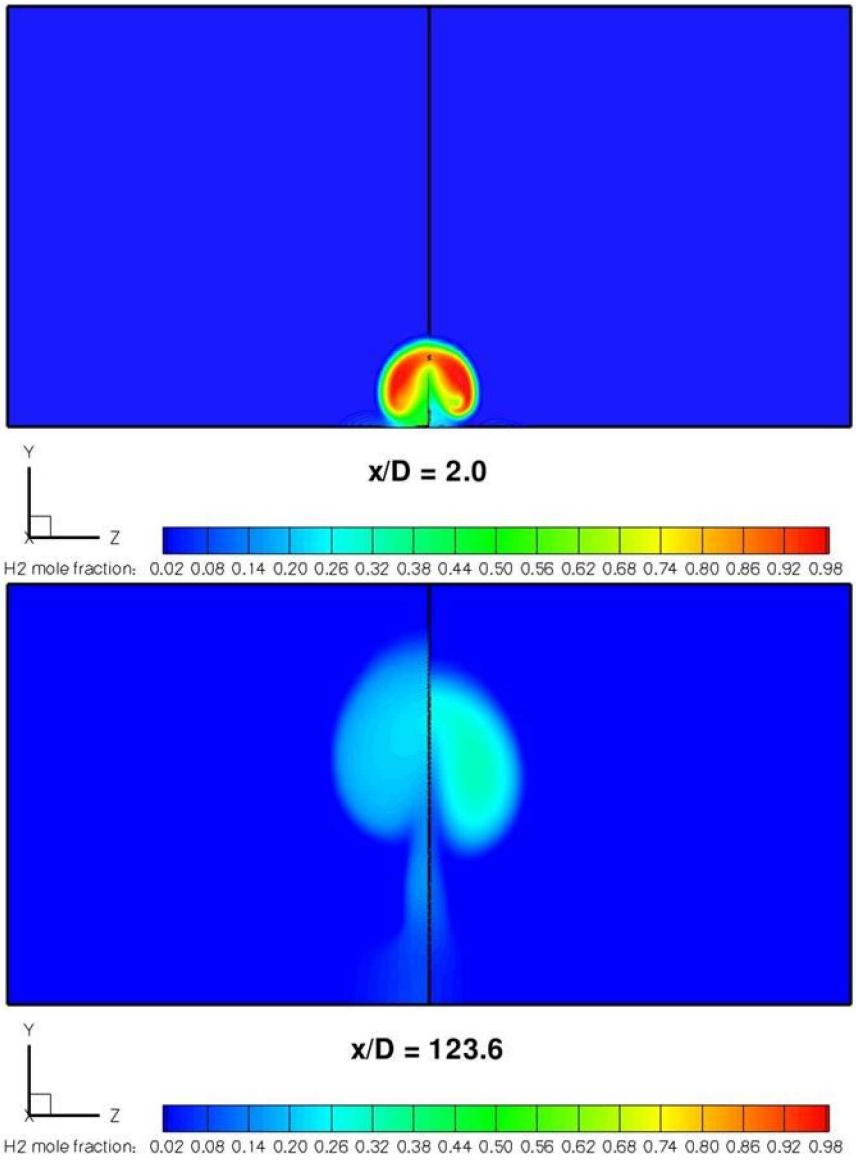

Figure 32. Sensitivity of the vented hydrogen mole fraction distribution to choice of turbulence Schmidt number (Sct = 0.25 - left of symmetry line, Sct = 1.0 - right of symmetry line).

As one would expect, the lower bound on the Schmidt number mixed out the plume to a greater extent than that given by the upper bound assumed for the Schmidt number. A similar analysis could have been performed to assess the sensitivity of the turbulent Prandtl number. However, the temperature difference between the plume and the exterior cross flow is minimal. Hence, the influence of the turbulent Prandtl number will be minimal when compared with the sensitivity to the turbulent Schmidt number shown here.

Finally, the effect of assumptions made to determine the vent condition are considered. The effects of changing the vented mass flow rate have previously been discussed. The

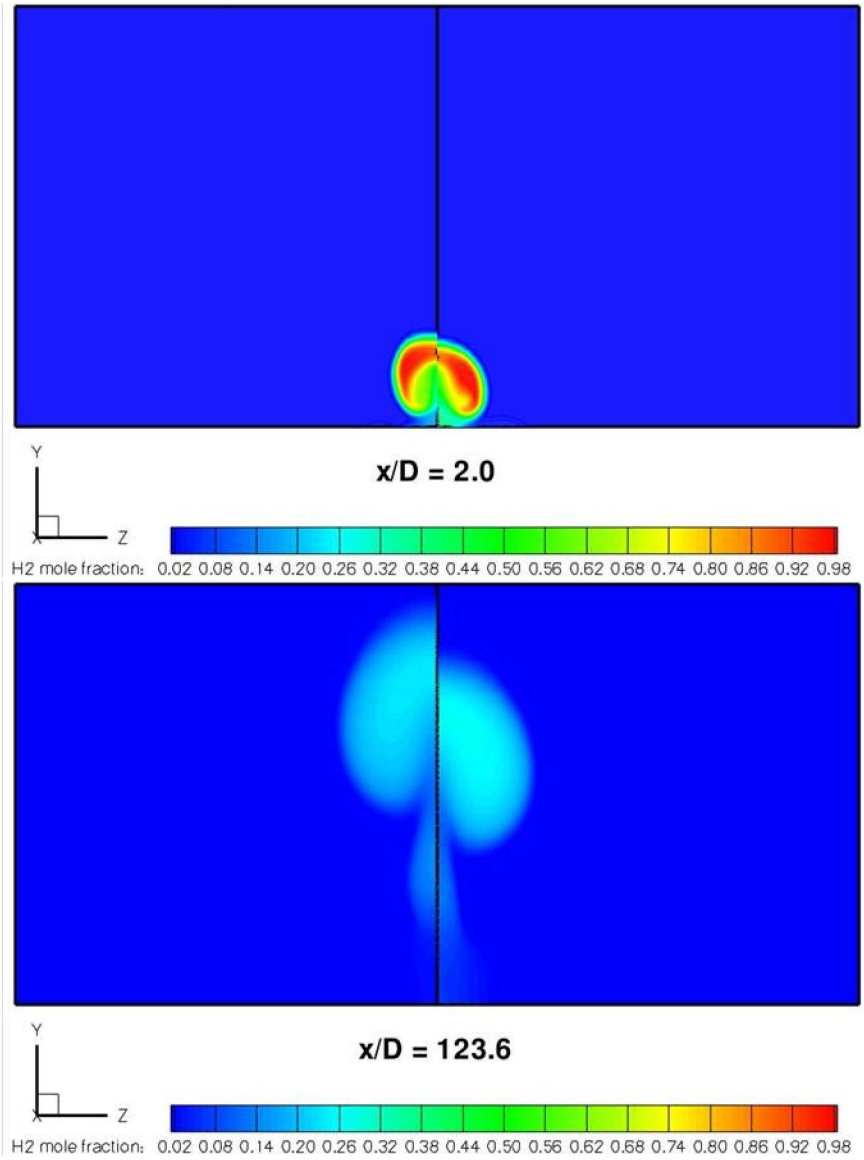

Figure 33. Sensitivity of the vented hydrogen mole fraction distribution to choice of vent condition (full isentropic expansion - left of symmetry line, choked at 5-inch exit - right of symmetry line).

present section considers the influence of the assumptions made as the flow traverses from the safety valve to the exit of the vent piping. Here there are essentially two bounding assumptions that can be made. The first assumption is that the flow chokes a second time at the exit of the 5-inch pipe section (followed by an isentropic expansion to the 7-inch exit plane). On the other end of the spectrum, one could assume that the entire expansion process from the safety valve to the exit of the 7-inch vent duct takes place isentropically. As noted previously, the first assumption appears to model the maximum vent flow rate cases reasonably well, but the isentropic assumption will become more valid

as the vent rate is reduced. To assess the sensitivity of the results to the assumptions made for the vent conditions, an additional simulation was performed that assumed isentropic expansions throughout the vent duct. The effect of vent condition is compared in Figure 33. A noticeable difference at the x/D=2.0 plane is evident with a change in vent condition. As expected, flow resulting from the isentropic expansion (which is absent of any total pressure losses) penetrates further into the freestream. This increase in penetration becomes even more evident as the plume traverses further downstream. Hence, care must be taken when assessing any particular valve failure mode to ensure that appropriate conditions have been specified at the vent exit plane.

5 Conclusions

This paper describes a series of studies to assess the potential risk associated with the failure of one of three gaseous hydrogen flow control valves in the orbiter's main propulsion system during the launch of Shuttle Endeavour (STS-126) in November 2008. The studies focused on critical issues associated with the possibility of combustion resulting from release of gaseous hydrogen from the external tank into the atmosphere during assent. The Shuttle Program currently assumes hydrogen venting from the external tank will result in a critical failure. The current effort is being conducted to increase understanding of the risk associated with venting hydrogen given the flow control valve failure scenarios being considered in the Integrated In-Flight Anomaly Investigation being conducted by NASA.

Analyses have indicated the gaseous hydrogen released following hydrogen flow control valve failure will mix with atmospheric air around the external tank and convect downstream as a combustible mixture that reaches the end of the external tank and the solid rocket booster plumes. Both the jet mixing analysis and the three-dimensional simulation produce this result. The simulations indicate that the hydrogen jet at maximum leak rate, following penetration through the boundary layer on the external tank, lies in the external flow beyond the boundary layer until it reaches the end of the tank and the SRB plume. As such, it would likely be impossible for combustion to propagate upstream from the plumes. At reduced flow rates, however, the hydrogen jet does not fully penetrate the boundary layer. A part of the resulting mixture then convects downstream at subsonic speeds. Applying the flashback analysis to both results, however, it appears that velocity gradients and the resulting strain on any flame in the flow field would result in the flame being extinguished and therefore unable to propagate upstream from the SRB plumes.

References

1. Dahm, Werner, Hydrogen Venting on Satern. Memo in Reply to Mr. Worlund, R-P&VE-PT-67-M-36-F, April 6,1967.

2. Seaford, Mark, Approximate Calculation of H2-Air Combustion Lengths During Shuttle Ascent. Data Compiled from External Tank Aeroheating Databook (SSD95D0489A), Section 3.1, "PE/SLWT No-Fail Baseline Aeroheating Trajectories." NASA Marshall Space Flight Center, March 17, 2009.

3. Baurle, Robert A., Details and additional information available from *r.a.baurle@nasa.gov* .

4. Kee, Robert J., Rupley, Fran M., Meeks, Ellen and Miller, James A., *CHEMKIN-III: A Fortran Chemical Kinetics Package for the Analysis of Gas-Phase Chemical and Plasma Kinetics.* Sandia National Laboratories, Report UC-405, SAND96-8216, May 1996.

5. Li, J., Zhao, Z., Kazakov, A., and Dryer, F.L. "An Updated Comprehensive Kinetics Model for H2 Combustion", Fall Technical Meeting of the Eastern States Section of the Combustion Institute, Pennsylvania State University, University Park, Pa, Oct 26-29, 2003.

6. Billing Fred S. , Orth, R. C., and Lasky, M., *A unified analysis of gaseous jet penetration*, AIAA Journal, Vol 9, No. 6, pp 1048-1058, 1971.

7. Norris, Andrew T., Details and additional information available from *andrew.t.norris@nasa.gov* .

8. Glassman, Irving, *Combustion*, Academic Press, Second edition, 1987.

9. Reynolds, W., STANJAN: Chemical Equilibrium Code, Stanford University, 1980

10. Pellett, G. L., Details and additional information available from *gerald.l.pellett@nasa.gov* .

11. Drell, Isadore L. and Belles, Frank E., *Survey of Hydrogen Combustion Properties*, NACA Report 1383, pp. 15-18, 1958.

12. Pellett, G. L., Isaac, K. M., Humphreys, W. M., Jr., Gartrell, L. R., Roberts, W. L., Dancey, C. L. and Northam, G. B., *Velocity and Thermal Structure, and Strain-Induced Extinction of 14 to 100% Hydrogen - Air Diffusion Flames*, Combustion and Flame **112**, No. 4, 1998.

13. Pellett, G. L., Vaden, S. N., and Wilson, L. G., Opposed Jet Burner Extinction Limits: Simple Mixed Hydrocarbon Scramjet Fuels vs. Air, AIAA Paper 2007-5664, July 2007.

14. Pellett, G. L., Vaden, S. N., and Wilson, L. G., Gaseous Surrogate Hydrocarbons for a HiFire Scramjet that Mimic Opposed Jet Extinction Limits for Cracked JP Fuels, JANNAF Paper 847, May 2008.

15. Hwang, Kyu C., Two Dimensional Numerical Simulation of Highly-Strained Hydrogen - Air Opposed Jet Laminar Diffusion Flames, PhD Dissertation, Old Dominion University, Norfolk, Virginia, May 2003.

16. Gomez, Reynaldo, Personal Communication. Shuttle surface velocity gradient calculations, Johnson Space Flight Center.

17. Gaffney, R. L., Details and additional information available from *richard.l.gaffney@nasa.gov*

18. Klippenstein, S. J., Personal Communication. Chemical Sciences and Engineering Division, Argonne National Laboratory

19. Hinze, J. O., *Turbulence*, McGraw-Hill, Second Edition, 1975.

20. Baurle, Robert A., VULCAN Users Manual, http://vulcan-cfd.larc.nasa.gov/, March 2009.

21. Wilcox, D. C., "Turbulence Modeling for CFD," DCW Industries, Inc.,2nd edition, 1998.

22. Menter, F. R., "Zonal Two Equation k-w Models for Aerodynamic Flows," AIAA Paper 93-2906, July 1993.

REPORT DOCUMENTATION PAGE

Form Approved
OMB No. 0704-0188

1. REPORT DATE *(DD-MM-YYYY)*	2. REPORT TYPE	3. DATES COVERED *(From - To)*
01-10-2009	Technical Memorandum	

4. TITLE AND SUBTITLE
Shuttle Gaseous Hydrogen Venting Risk from Flow Control Valve Failure

5a. CONTRACT NUMBER

5b. GRANT NUMBER

5c. PROGRAM ELEMENT NUMBER

6. AUTHOR(S)
Drummond, J. Philip; Baurle, Robert A.; Gaffney, Robert L.; Norris, Andrew T.; Pellett, Gerald L.; Rock, Kenneth E.

5d. PROJECT NUMBER

5e. TASK NUMBER

5f. WORK UNIT NUMBER
378343.10.01.05.08

7. PERFORMING ORGANIZATION NAME(S) AND ADDRESS(ES)
NASA Langley Research Center
Hampton, VA 23681-2199

8. PERFORMING ORGANIZATION REPORT NUMBER
L-19767

9. SPONSORING/MONITORING AGENCY NAME(S) AND ADDRESS(ES)
National Aeronautics and Space Administration
Washington, DC 20546-0001

10. SPONSOR/MONITOR'S ACRONYM(S)
NASA

11. SPONSOR/MONITOR'S REPORT NUMBER(S)
NASA/TM-2009-215942

12. DISTRIBUTION/AVAILABILITY STATEMENT
Unclassified - Unlimited
Subject Category 34
Availability: NASA CASI (443) 757-5802

13. SUPPLEMENTARY NOTES

14. ABSTRACT

This paper describes a series of studies to assess the potential risk associated with the failure of one of three gaseous hydrogen flow control valves in the orbiter's main propulsion system during the launch of Shuttle Endeavour (STS-126) in November 2008. The studies focused on critical issues associated with the possibility of combustion resulting from release of gaseous hydrogen from the external tank into the atmosphere during assent. The Shuttle Program currently assumes hydrogen venting from the external tank will result in a critical failure. The current effort was conducted to increase understanding of the risk associated with venting hydrogen given the flow control valve failure scenarios being considered in the Integrated In-Flight Anomaly Investigation being conducted by NASA.

15. SUBJECT TERMS
Shuttle; Safety; Combustion; Fluid mechanics

16. SECURITY CLASSIFICATION OF:			17. LIMITATION OF ABSTRACT	18. NUMBER OF PAGES	19a. NAME OF RESPONSIBLE PERSON
a. REPORT	b. ABSTRACT	c. THIS PAGE			STI Help Desk (email: help@sti.nasa.gov)
					19b. TELEPHONE NUMBER *(Include area code)*
U	U	U	UU	42	(443) 757-5802